# Granular flow properties of food powders in extrusion processing

by

Cameron McGuire

B.S., Kansas State University, 2014

A THESIS

Submitted in partial fulfillment of the requirements for the degree

MASTER OF SCIENCE

Department of Grain Science
College of Agriculture

KANSAS STATE UNIVERSITY
Manhattan, Kansas

2017

Approved by:

Major Professor
Dr. Sajid Alavi

# Copyright

# Abstract

This study relates raw material particulate rheology to the granular flow in a single screw food extruder. Raw materials based on corn (i.e. meal, flour, and starch), wheat (i.e. farina, flour and starch), and sucrose (i.e. granulated, superfine, and powdered) were used as model particulate systems for the study. Various particulate-scale characteristics and flow parameters of these nine materials were determined using a powder rheometer. Properties such as basic flow energy, cohesion, flow function, and effective angle of internal friction were good indicators of flowability in an extruder. Corn meal exhibited lower energy requirements and a higher propensity for flow than corn flour (6.7mJ/g versus 10.7mJ/g, and "free-flowing" versus "cohesive," according to Flow Function classifications), with wheat farina showing similar results when compared to wheat flour (5.8mJ/g versus 7.9mJ/g, and "highly free-flowing" versus "cohesive"), although both wheat systems showed lower energy requirements than their comparable corn systems. Sugar, being of a different base material and particle shape, behaved differently than these starch-based materials—flow energy decreased and propensity to flow increased as particle size decreased (51.7mJ/g versus 8.0mJ/g, and "free-flowing" versus "highly free-flowing"). This large energy requirement for coarse sugar particles was attributed more to particle shape than composition, as the sharp edges of sugar can interlock and restrict movement through the sample. The starch-based results were validated in a particulate flow study involving the above model systems (corn meal, corn flour, wheat farina, and wheat flour) in a pilot-scale single screw extruder. Visualization data, obtained using a transparent plexiglass window during extrusion, confirmed that the

flours exhibited higher flow energy requirements and a lower flow factor compared to coarser-particle size during extrusion, seen by the increased peak heights and barrel fill.

Additionally, moisture changes were analyzed, showing an increase in energy required for starch-based materials as moisture increases and a decrease in energy for sucrose. Due to the hygroscopic nature of sucrose, moisture was absorbed more rapidly than starch products and the edges of individual particles softened, forming a soft solid. These physiochemical differences resulted in decreased energy requirements for sucrose as moisture was increased (51.7mJ/g to 13.6mJ/g), while corn meal and wheat farina yielded increased energy requirements (6.7mJ/g to 9.1mJ/g and 5.8mJ/g to 9.5mJ/g, respectively). Again, results of starch-based materials were validated using a plexiglass cover during extrusion, clearly showing an increase in barrel fill as moisture content increased for both materials, with corn meal flowing more readily than farina.

Lastly, temperature of corn meal and farina was increased to show the difference in behavior of starch-based materials, where farina decreased in energy as temperature increased (14.4mJ/g to 12.1mJ/g ) while corn meal energy requirements increased (12.9mJ/g to 17.2mJ/g).

With the results developed from these three experiments, and validated where physically possible, it was concluded that offline powder rheometry is a useful tool for predicting the behavior of food powders. These results were then developed into a computer-simulated model to allow for virtual and visual representation of the conveying action inside an enclosed steel barrel.

# Table of Contents

# List of Figures

# List of Tables

# List of Equations

# List of Abbreviations

| | |
|---|---|
| AIF(E) | Effective Angle of Internal Friction (°) |
| BFE | Basic Flow Energy (mJ) |
| C.Flour | Corn Flour |
| C.Meal | Corn Meal |
| COR | Coefficient of Restitution |
| CORF | Coefficient of Rolling Friction |
| COSF | Coefficient of Static Friction |
| FE | Flow Energy (mJ) |
| FF | Flow Function |
| FRI | Flow Rate Index |
| MC | Moisture Content |
| MPS | Major Principle Stress (kPa) |
| SE | Specific Energy (mJ/g) |
| SI | Stability Index |
| SBFE | Specific Basic Flow Energy (mJ/g) |
| UYS | Unconfined Yield Strength (kPa) |
| WFA | Wall Friction Angle (°) |
| W.Farina | Wheat Farina |
| W.Flour | Wheat Flour |

# Acknowledgements

Thank you to my advisor, Sajid Alavi, for introducing me to the world of extrusion, for the opportunity to take on a project of this magnitude, and for challenging me to grow both academically and professionally.

Thank you, also, to my committee members Drs. Kingsly Ambrose and Ronaldo Maghirang for dedicating their time and sharing their insight to further improve my research methods and my critical thinking skills through these experiments.

I also want to thank Eric Maichel and his team at Extrusion Lab 17 at Kansas State University for their assistance in the operation of the extruder and gathering measurements during the inline validation studies.

Lastly, thank you to my parents for instilling a love of learning in me at a young age, and my family for their continuous support—without them, my academic career would never have become so rich.

# Chapter 1 - Introduction

While extrusion technology has been around for millennia, only in recent decades has extrusion been used for food production. Since this debut into food applications, extrusion processing has developed into an extremely versatile system that can be used to create a wide array of products—from puffed snacks and breakfast cereal to pet food and aquatic feed. Food extrusion is typically based on a starch matrix for structure, achieved by utilizing raw materials such as corn, wheat, or sorghum meals/flours, but other protein or fiber sources can be added, acting as fillers throughout the starch matrix. Each material added has a nutritional, palatability, or functional goal, which can also have a positive or negative impact on flowability through the extruder based on its composition. During extrusion, material is not just conveyed from the inlet feed out through the opposite end. Instead, increasing pressure and temperatures along the length of the barrel, along with the rotation of the screw, result in mixing, kneading, melting, and cooking of the material prior to exiting the die. Broadly speaking, there are three main processing zones in an extruder barrel, where material undergoes physical and chemical transformations. These zones, illustrated in Figure 1-1, are:

1. Feeding/metering zone, where the raw granular material is fed into the barrel at atmospheric pressure. An increase in temperature or surface moisture may be observed due to preconditioning of the material prior to entering the extruder, which will result in a loosely-agglomerated particle flow;
2. Kneading/transition zone, where the loose particles begin to compact and temperature increases, transforming the material into a dough-like mass with addition of water and/or steam; and

3. Cooking zone, where temperatures and pressures drastically increase due to restriction of flow caused by the comparatively-small die size at the exit point, turning the dough into a fluidized melt (Riaz 2000).

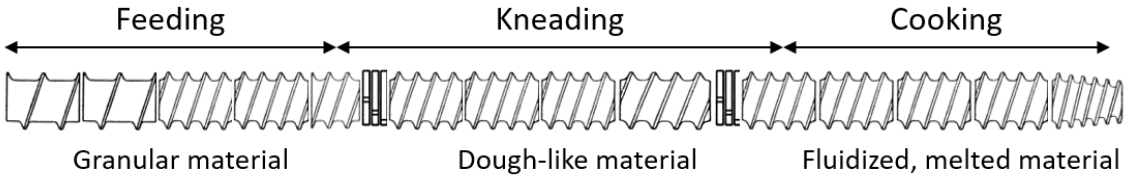


**Figure 1-1 Extruder Screw Zones**

## 1.1 Objectives

The scope of this paper focuses on the feeding zone of the extruder with granular flow of food powders as they enter and travel through this zone. The main objectives of study were as follows:

1. To develop an offline understanding of how food powders of three different compositions and three different particle sizes (in a full-factorial design) flow
2. Develop an offline understanding of moisture content increases to flow properties of coarse food powders.
3. Develop an offline understanding of temperature increase to flow properties of coarse, starch-based food powders.
4. Validate offline results through inline trials, and develop DEM simulations based around these results.

# Chapter 2 - Particle Size and Composition of Food Powders in Extrusion


## Abstract

Innovations in food extrusion technology are enabling its rapid expansion and applicability in diverse areas related to bioprocessing and value addition. This study relates raw material particulate rheology to the granular flow in a single screw food extruder. Raw materials based on corn (i.e. meal, flour, and starch), wheat (i.e. farina, flour and starch), and sucrose (i.e. granulated, superfine, and powdered) were used as model particulate systems for the study. Various particulate-scale characteristics and flow parameters of these nine materials were determined using a powder rheometer, a promising new offline tool. Properties such as basic flow energy, specific energy, cohesion, stability index, flow function, and effective angle of internal friction were good indicators of flowability in an extruder. Corn meal exhibited lower energy requirements and a higher propensity for flow than corn flour (6.7mJ/g versus 10.7mJ/g, and "free-flowing" versus "cohesive," according to Flow Function classifications), with wheat farina showing similar results when compared to wheat flour (5.8mJ/g versus 7.9mJ/g, and "highly free-flowing versus "cohesive," according to Flow Function classifications), although both wheat systems showed comparatively lower energy requirements than their comparable corn systems. Sugar, being of a different base material and particle shape, behaved differently than these starch-based materials—flow energy decreased and propensity to flow increased (51.7mJ/g versus 8.0mJ/g, and "free-flowing" versus "highly free-flowing"). This large energy requirement for coarse sugar particles may be attributed more to particle shape than composition, as the sharp edges of sugar can

interlock and increase restriction to movement through the sample. The starch-based results were validated in a particulate flow study involving the above model systems (corn meal, corn flour, wheat farina, and wheat flour) in a pilot-scale single screw extruder. Visualization data, obtained using a transparent plexiglass window during extrusion, confirmed that the flours exhibited higher flow energy requirements and a lower flow factor when compared to the coarser-particle size corn meal during extrusion, seen by the increased peak heights and barrel fill.

## 2.1 Introduction

In extrusion processing, material starts in a hopper, is fed through a feeder screw, through a preconditioning system and finally into the extruder. All of this flow takes place as a granular material; it is not until the material enters the kneading and cooking zones that it undergoes pressure and temperature changes that begin to transition the powder into a fluidized mass before exiting the die at the end of the barrel.

While this is a simplified illustration of an extrusion system and each target product has different optimal processing parameters—moisture added, thermal energy added, screw profile, barrel temperature, etc.—the zones, and physiochemical changes that occur in these zones, are always present. Analysis of flow and cook patterns changes with each zone, as the material changes from individual granules to a compacted solid to a viscous melt, but the understanding of these patterns leads to improved developments of screw configuration, screw/barrel metallurgy, and operational parameters. In the feeding zone, specifically, understanding the behavior of particle flow as a function of size and composition is the key to these developments. As extrusion occurs in an enclosed system with forward movement aided by a rotating screw, particle-surface interactions play a

significant role in flow, in addition to interparticle forces. Flowability is a result of physical, chemical, and environmental variables, meaning factors such as wall friction, powder cohesiveness, and angle of internal friction, along with many others, are key components that determine how efficiently a material conveys from the start of the barrel into the kneading and cooking zones (Freeman 2000). If a material will not flow well upon entering the feeding zone, the entire process can back up, choking the extruder and resulting in time lost due to clearing the blockage. Even if a material flows, a blended mixture may have components that behave differently—one element being more adhesive to the barrel surface and another agglomerating to like particles more—so it is important to understand how the individual, raw materials of a product will behave to proactively anticipate system performance.

Beyond the particle-wall interactive forces present in this system, additional factors impact the effectiveness of material flow, such as particle shape. Yamane et al. (1998) performed discrete element modeling on the dynamic angle of repose of non-spherical mustard seeds compared to spherical particles, with the non-spherical particles showing a greater angle of repose at any given rotational speed of a drum. These results were also found by Dury and Ristow (1998), where two species of mustard seed were compared against spherical glass beads rotated in a drum, and an increased coefficient of friction was observed for both varieties of non-spherical seeds over the spherical beads. Additionally, particles that are irregularly shaped, with sharp corners or other non-rounded sides/edges have even higher angles of internal friction than lenticular or ellipsoidal particles due to their ability to interlock and subsequently resist flow action (Juliano 2006).

Composition of the material contributes to flow patterns, as well—starch-based, protein-based, and sucrose-based powders all have roles in extrusion processing for the end product, and each have different flow properties and limitations. Fitzpatrick et al. (2003) analyzed flow functionality of one dozen food powders of similar [fine] particle sizes and found the flow index was influenced by composition (including equilibrium moisture), although angle of internal friction and wall friction angles did not directly correlate, which indicates the factors mentioned previously do, in fact, modify flow in different ways depending on the aspect being analyzed—particle-wall, particle-particle in terms of cohesion or angle of internal friction, or overall flowability in confined space.

### *2.1.1 Objectives*

1. Explore correlation between flow functionality, energy requirements as particle size increases for food powders based on corn, wheat, and sucrose.
2. Explore correlation between flow functionality, energy requirements as composition of food powder changes between corn, wheat, and sucrose for given particle size range, relative to the scope of the experiment—coarse, medium, and fine.

## 2.2 Materials and Methods

### *2.2.1 Materials*

The materials used for this experiment were as follows: Corn Starch (Argo, Engelwood Cliffs, NJ), corn flour (Bunge, Atchison, KS), corn meal (Aunt Jemima, Chicago, IL), wheat starch (MGP Ingredients, Atchison, KS), wheat flour (Gold Medal, Minneapolis, MN), wheat farina (Hal Ross Mill, Kansas State University, Manhattan,

KS), powdered sugar (C&H, Yonkers, NY), superfine sugar (C&H, Yonkers, NY), and granulated sugar (C&H, Yonkers, NY).

*2.2.2 Particle Size Measurement*

Preliminary particle size was measured via Rotap sieve stack. The stack of sieves used contained screen openings of [841µm, 594µm, 420µm, 297µm, 212µm, 125µm, 73µm, and a pan (0µm)]. Using log diameter of screen size multiplied by mass of particles on the screen, a particle size distribution was developed, with an average particle size calculated from the distribution. The equation is given in Equation 2-1.

$$\boldsymbol{Average\ Particle\ Size} = \mathbf{10}^{\frac{\sum((mass\ on\ screen)*\log(screen\ opening))}{\sum(mass\ on\ screen)}} \quad \textbf{(2-1)}$$

Laser diffraction—using a Malvern Mastersizer 3000—was also used to measure particle size as a more accurate method than the preliminary Rotap and equation. This process infers particle volume based on light diffraction of particles as they move past the window, through the path of the laser beam transmission. Detectors in various positions throughout the apparatus are used to estimate diffraction patters for individual particles. Concentration of particles for testing ranged from 0.0020%-0.0471%, to reduce particle agglomeration and clouding of the detection window.

*2.2.3 Moisture Testing*

AOAC Moisture Method 930.15 was employed for all samples, in triplicate, to ascertain moisture content using a conventional drying oven at 135°C for 2 hours.

*2.2.4 Equipment and Testing Methods*

The Freeman Technology FT4 Powder Rheometer was used to perform four powder property tests: Stability and Variable Flow Rate, Compressibility, Shear Cell, and Wall Friction, outlined in the following subsections.

*2.2.4.1 Stability and Variable Flow Rate*

A 160mm x 50mm glass cylinder was mounted onto the testing base, connected to a smaller 85mm x 50mm cylinder on top, with a funnel. This was tared before being filled with the powder to be analyzed, providing the mass of the powder to be incorporated into results. For this test, a 48mm helical blade conditioned the sample by traversing down and up 2 times before the material in the top cylinder was removed to leave a standard volume of product for subsequent measuring. After the vessel splitting, the new, conditioned mass was recorded, and the testing cycles began. The standard dynamic test consisted of seven test cycles (tests 1 to 7) at a blade tip speed of 100mm/s with counterclockwise motion while traversing through the granular material from top to bottom, and clockwise motion while retracting back to the top. These identical test cycles were performed to achieve stabilization of flow energy and characterize change in flow behavior due to attrition, agglomeration, segregation, etc. Subsequently, four more test cycles were conducted (tests 8 to 11) with blade tip speed gradually decreasing (100 mm/s, 70 mm/s, 40 mm/s and 10 mm/s, respectively), in order to evaluate sensitivity to different flow rates. The results given utilized the energy requirements from the various cycles to calculate powder characteristics.

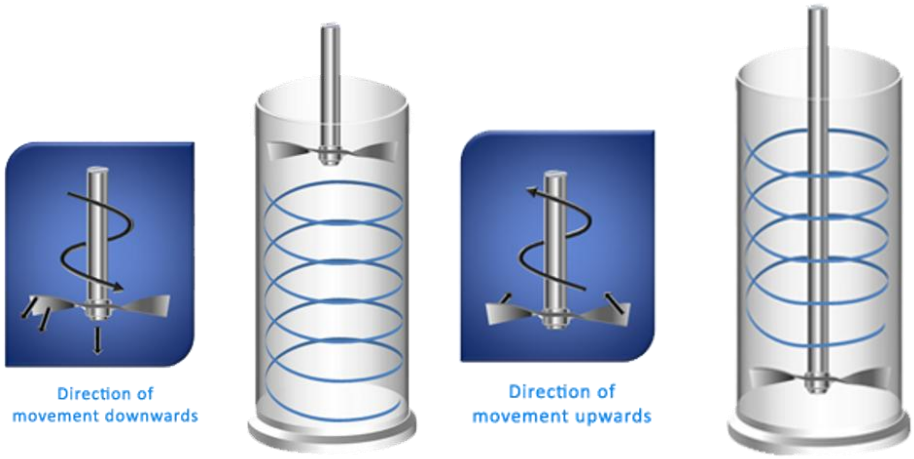


**Figure 2-1 Rotation of helical blade during testing**

**Figure 2-2 Splitting vessel after conditioning**

Basic Flowability Energy (BFE) is the total energy used for the blade to traverse downward in the seventh cycle of the testing process, which represents confined flow (as the blade moved toward the base of the container, meeting resistance). The higher this value, the more energy required for this cycle, with the following equation:

$$BFE\ (mJ)\ =\ \int_0^{\Delta x}(T\dot{\theta} + Fv_x)v_x^{-1}dx \qquad \textbf{(2-2)}$$

Where:
T = rotation resistance or torque experienced by the blade (N·m)
F = vertical resistance or force experienced by the blade (N)
$\dot{\theta}$ = angular speed of the blade (rad/s)
$v_x$ = vertical speed of the blade (m/s)
$\Delta x$ = vertical distance traversed by the blade

Specific Basic Flow Energy (SBFE) is BFE divided by total mass of product in the cylinder to give Joules/gram, which allows for a more uniform comparison across products with different densities, as formulations for products are mixed on a per-mass basis, not per-volume basis.

In contrast to BFE, Specific Energy (SE) represents the energy taken to move from the base of the cylinder to the top, representing unconfined flow, and divided by the mass of the sample to give a per-unit-mass value in Equation 2-3.

$$SE\ (mJ/g)\ = \frac{(FE_6+FE_7)/2}{m} \tag{2-3}$$

Where:
$FE_6$ = Upward flow energy required during test cycle 6 (mJ)
$FE_7$ = Upward flow energy required during test cycle 7 (mJ)
m = Mass of sample (g)

Stability Index shows whether a powder expands, compacts, or remains at the same volume through the test cycles. A value near 1.00 indicated the powder maintains its volume, while a value greater or less than 1.00 indicated the powder had a tendency to compact or expand, respectively. This value was calculated using Equation 2-4:

$$SI = \frac{BFE_7}{BFE_1} \tag{2-4}$$

Where:
$BFE_1$ = Flow energy required during test cycle 1
$BFE_7$ = Flow energy required during test cycle 7.

Finally, Flow Rate Index (FRI) is the factor by which flow energy is changed when the blade tip speed is reduced by a factor of 10. It evaluates the sensitivity of the powder to different flow rates, and is calculated as follows:

$$FRI = \frac{BFE_{11}}{BFE_8} \tag{2-5}$$

Where:
$BFE_8$ = Flow energy required during test cycle 8 and
$BFE_{11}$ = Flow energy required during test cycle 11.

*2.2.4.2 Compressibility*

For the Compressibility test, the same 48mm helical blade was used to condition the sample, with a glass cylinder of 85mm x 50mm used for the base. After the conditioning cycle was completed, the blade was replaced by a 48mm-diameter vented piston. The top cylinder was split to remove excess powder, leaving a standard volume of product, and then the piston was lowered at increasing force levels—0.5, 1, 2, 4, 6, 8, 10, 12, 15kPa—and the percentage compression of the powder was recorded at each force interval. These force/compression results were plotted on a graph internally and presented at the completion of the test.

*2.2.4.3 Shear Cell*

Testing of shear properties allows for further understanding of the inter-particulate forces that powders are subjected to during handling and processing, such as the yield point of powder flow initiation. Preparation for the Shear Cell test involved using the 48mm helical blade, followed by the 48mm diameter vented piston, and then splitting the two 85mm x 50mm glass cylinders, leaving a compacted volume of sample for the test. The shear cell attachment, with the same radius as the vented piston but with small blades on the underside, was used to carry out the test by inducing rotational and vertical stress. Once the powder bed in the cylinder yielded to the stress applied by the shear head, the stress value was recorded.

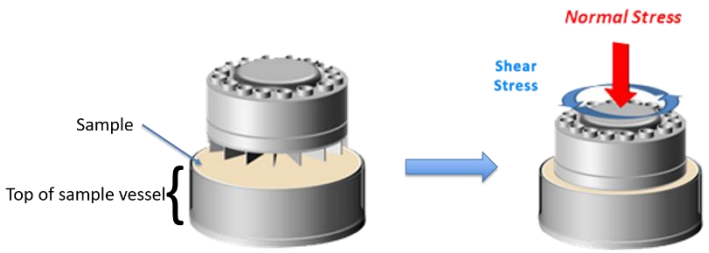


**Figure 2-3 Shear Cell head**

These results utilized the Mohr Circle analysis to calculate values such as Cohesion, Major Principle Stress, Unconfined Yield Strength, and Flow Factor, illustrated in Figure 2-9. Test points were plotted along a graph to determine Cohesion factor (y-intercept value of yield locus—line through data points) and Effective Angle of Internal Friction (angle of line drawn between farthest test point and origin compared to x-axis). Unconfined Yield Strength (UYS) was developed by drawing a half-circle from the origin, tangent to the yield locus, and the point the half-circle crossed the x-axis was labeled as the UYS. Major Principal Stress (MPS) was calculated in a similar matter, with a semi-circle drawn between the farthest test point and the pre-shear point, with the higher end of the semi-circle labeled as the MPS.

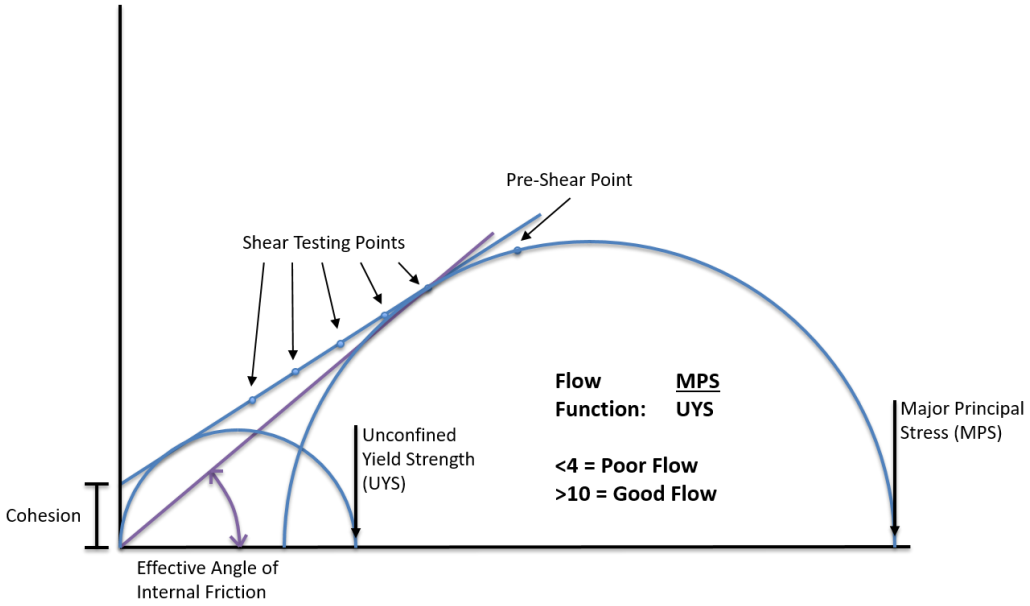


**Figure 2-4 Typical Mohr Circle plot**

Flow Function (FF) was calculated using Equation 2-6 (Jenike 1961), which directly indicates how easily a powder will flow, with a higher value indicating a greater propensity to flow and a lower number indicates a resistance to flow. These values have

been elaborated on by Thomas and Schubert (1979) and divided into categories seen in Table 2.1.

$$FF = \frac{MPS}{UYS} \tag{2-6}$$

**Table 2.1 Classification of Particulate Flowability Based on Flow Function Value**

| Type of Flow | Flow Function Value |
|---|---|
| Not Flowing | FF < 1 |
| Very Cohesive | 1 < FF < 2 |
| Cohesive | 2 < FF < 4 |
| Easy-Flowing | 4 < FF < 10 |
| Free-Flowing | 10 < FF |

*2.2.4.4 Wall Friction*

This test measures the resistance of flow of powders in relation to the process equipment surface by using a friction disc head that applies both vertical and rotational stress on a powder at rest to determine the torque necessary to overcome the resistance of the powder bed. Preparation for the Wall Friction test involved using the 48mm helical blade, followed by the 48mm diameter vented piston, and then splitting the two 85mm x 50mm glass cylinders, leaving a compacted volume of sample for the test. A Wall Friction disc, with a friction coefficient value of 0.05 (low friction interference), was used for the test.

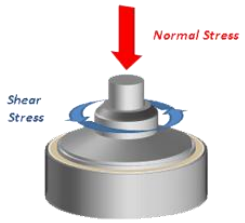


**Figure 2-5** Wall Friction head

The torque required to maintain the rotational momentum of the disc was measured and used to calculate a 'steady-state' shear stress. The normal stress was maintained at a constant value throughout the measurement. From the relationship between normal stress ($\sigma_w$) and shear stress ($\tau_w$), the wall friction angle ($\phi$), is calculated as follows:

$$\phi = tan^{-1}\left(\frac{\tau_w}{\sigma_w}\right) \tag{2-7}$$

## 2.3 Results and Discussion

### *2.3.1 Particle Size*

Utilizing the equation given in (2-1), average particle size for each material was determined to be: corn starch (12 μm), corn flour (154 μm), corn meal (622 μm); wheat starch (23 μm), wheat flour (72 μm), wheat farina (410) μm); powdered sugar (12 μm), superfine sugar (150 μm), and granulated sugar (450 μm).

Testing from the Malvern Mastersizer 3000 yielded the following average particle size for the nine materials in this experiment: corn starch (13.6 μm), corn flour (94.2 μm), corn meal (616 μm); wheat starch (29.9 μm), wheat flour (71.3 μm), wheat farina (425) μm); powdered sugar (23.4 μm), superfine sugar (151 μm), and granulated sugar (438 μm).

Since food particles are a variety of shapes, there is error associated with the assumption that all particles are spherical. The diversity of shapes also creates error in sieve measurements, as a long skinny particle may or may not pass through a screen opening, depending on its orientation. If it passes through an opening when it orients vertically, it is counted as being smaller than if it had not bounced to that orientation, thus

remaining on the larger sieve screen. However, due to the close values between the Malvern Mastersizer and the Rotap, these potential errors do not seem to have impacted the results.

### *2.3.2 Moisture Content*

Moisture content for each material was found to be as follows: corn starch, 10.32%; corn flour, 11.04%; corn meal, 13.13%; wheat starch, 9.40%; wheat flour, 12.28%; wheat farina, 13.73%; powdered sugar, 0.38%; superfine sugar, 0.09%; and granulated sugar, 0.06%.

### *2.3.3 Corn Particle Size*

Stability and variable flow rate testing show that, as particle size increases, energy requirements for confined and unconfined flow decrease. The increase in energy with smaller particles can be attributed to an increase in surface area that increases interparticle friction, resisting the flow of the blade. The results of the stability index show that corn flour and corn starch both compact during the testing, while corn meal slightly expands as the blade rotates through the sample. The flow rate index shows that corn starch is more sensitive to changes in blade speed when compared to corn flour and corn meal.

**Table 2.2 Stability Results for Corn Powders**

| Sample | SBFE | SE | SI | FRI |
|---|---|---|---|---|
| Corn Starch | $11.01\pm0.08^{A}$ | $12.93\pm1.19^{A}$ | $1.18\pm0.03^{A}$ | $1.61\pm0.04^{A}$ |
| Corn Flour | $10.71\pm0.05^{B}$ | $8.36\pm0.09^{B}$ | $1.07\pm0.04^{B}$ | $1.38\pm0.01^{B}$ |
| Corn Meal | $6.70\pm0.00^{C}$ | $3.37\pm0.10^{C}$ | $0.97\pm0.01^{B}$ | $1.40\pm0.02^{B}$ |

The shear testing, performed under constant rotational stress, yielded results that were different than visual observations. Corn starch, according to the test, is a free-flowing powder with a Flow Function value >10 and a lower angle of internal friction. However, this result may be attributed to the constant stress the powders are under during testing—once corn starch (or any material) is under enough constant pressure, it fluidizes and results in the inflated values that reflect a free-flowing liquid. While Marston et al. (2012) found that decreasing particle size of materials resulted in behavior more similar to water when struck with a solid object at a constant velocity, specific values for fluidization were not found. This does explain the variation from expected results, while also providing insight to the problems observed in extrusion processing. Corn starch is known for subjectively not flowing well in an extruder, but with these results and the knowledge provided from work done by Marston, the reason why may be different than originally thought. The addition of water or oil in production of extruded products reduces the mechanical energy input in the system due to the lubricating effects of the liquids, causing slippage and resistance to forward flow encouraged by the screw. If corn starch fluidizes in the barrel, the reduced flowability is not due to a cohesive resistance to flow (like that seen with corn flour) but is, instead, due to the high propensity to flow of the material. This flow would cause slippage and prevent the conveying action of the screw, resulting in increased barrel fill due to the lack of material exiting through the die.

**Table 2.3 Shear Results for Corn Powders**

| Sample | Cohesion | MPS | UYS | FF | AIF(E) |
|---|---|---|---|---|---|
| Corn Starch | $0.440\pm0.099^{C}$ | $23.20\pm0.15^{A}$ | $1.93\pm0.04^{C}$ | $12.03\pm0.26^{A}$ | $34.1\pm0.2^{C}$ |
| Corn Flour | $1.797\pm0.073^{A}$ | $20.43\pm0.09^{B}$ | $8.67\pm0.30^{A}$ | $2.36\pm0.07^{C}$ | $58.5\pm0.3^{A}$ |
| Corn Meal | $0.843\pm0.051^{B}$ | $19.73\pm0.09^{C}$ | $4.02\pm0.22^{B}$ | $4.94\pm0.27^{B}$ | $49.0\pm0.1^{B}$ |

Cohesion values tended to relate to yield stress, flow function, and angle of internal friction. The greater the cohesion value a powder has, the more the particles interact with each other, which results in a higher yield strength, lower flow function, and greater angle of internal friction.

Cohesive powders have interparticle forces that create bridges and void spaces in a given volume, whereas non-cohesive powders tend to flow freely to occupy as much of a given volume as possible. The latter results in very little compressibility due to the lack of void space available for particles to nestle into when force is applied. The former, however, has much more space (further increasing as cohesiveness increases) that allow for particles to compact into, resulting in increasing compressibility in tandem with increasing cohesive properties (Peleg 1973).

The results below showed a correlation to the cohesion factor for corn flour, alone, as it had the highest cohesion value and was compressed the most. However, corn meal was shown to be more cohesive but less compressible than corn starch, despite having a higher cohesion value. These results contribute to the hypothesis that the constant rotational stress in the previous test fluidized corn starch and yielded artificially lowered results.

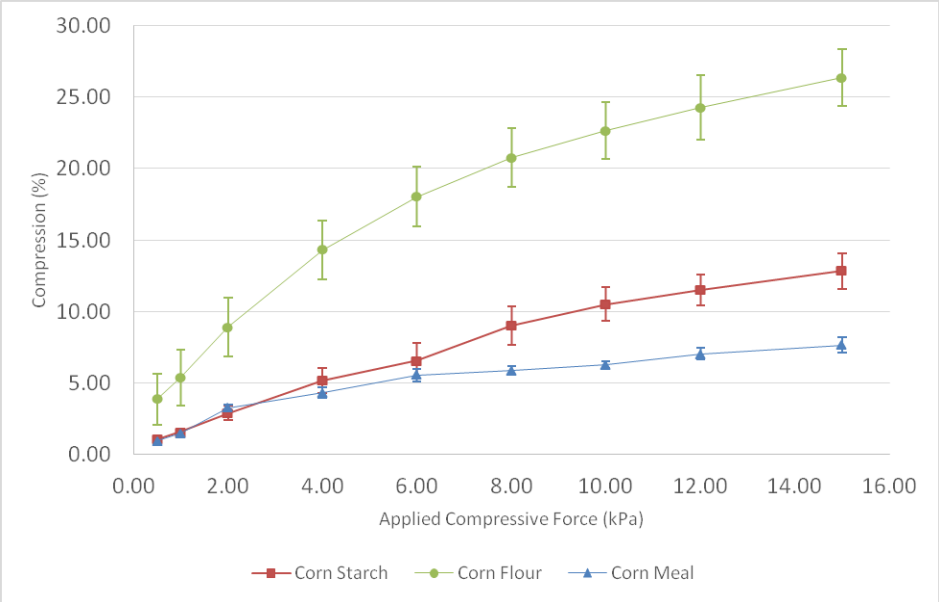


**Figure 2-6 Compressibility results of Corn powders**

The wall friction testing showed that the wall friction angle decreases as particle size increases. A greater decrease in the angle is seen between corn starch to corn flour than from corn flour to corn meal, similar to the cohesion value in the shear testing. This may indicate a relationship between cohesion and wall friction—an increase in interparticle forces results in a decrease in the impact of external forces, such as friction from a wall.

**Table 2.4 Wall Friction Results of Corn Powders**

| Sample | WFA |
|---|---|
| Corn Starch | $13.1 \pm 0.5^{A}$ |
| Corn Flour | $7.7 \pm 0.2^{B}$ |
| Corn Meal | $5.8 \pm 0.1^{C}$ |

*2.3.4 Wheat Particle Size*

Similar to corn products, stability and variable flow rate testing show that energy requirements for confined and unconfined flow decrease as particles size increases. The flow rate index shows that wheat starch was more sensitive to changes in blade speed when compared to wheat flour or wheat farina. With a FRI value of <1.0 for farina, it can be inferred that a slower blade speed is more energy efficient for moving through the particles. This could be due to the shape of the particles, as the Stability Index of 1.0 indicates that farina tends to neither compact nor expand throughout the testing process. Contrarily, the starch and flour powders settled and compacted during the conditioning of the test and required noticeably more energy when blade speed was reduced for Flow Rate Index testing.

**Table 2.5 Stability Results of Wheat Powders**

| Sample | SBFE | SE | SI | FRI |
|---|---|---|---|---|
| Wheat Starch | $14.24\pm0.11^{A}$ | $8.64\pm0.26^{A}$ | $1.07\pm0.03^{AB}$ | $1.63\pm0.01^{A}$ |
| Wheat Flour | $7.94\pm0.08^{B}$ | $6.50\pm0.85^{B}$ | $1.12\pm0.03^{A}$ | $1.21\pm0.01^{B}$ |
| Wheat Farina | $5.81\pm0.09^{C}$ | $2.66\pm0.01^{C}$ | $1.00\pm0.00^{B}$ | $0.95\pm0.01^{C}$ |

As the wheat starch used was a coarser particle size than native wheat starch granules are, the product was more free-flowing than anticipated. The correlations with cohesion and other values are still present, however, with Flow Factor being much higher if a low cohesion value was reported. Lower UYS and AIF(E) were also seen with low cohesion, which both starch and farina showed. Flour, with a cohesion value close to four times that of starch and farina, exhibited a much higher UYS, a noticeably higher AIF(E),

and was much more resistant to flow with a FF value of 3.3. This value classifies it as a "cohesive flow," while starch is "free-flowing," and farina is "highly free-flowing."

**Table 2.6 Shear Results of Wheat Powders**

| Sample | Cohesion | MPS | UYS | FF | AIF(E) |
|---|---|---|---|---|---|
| Wheat Starch | $0.468\pm0.048^{B}$ | $16.93\pm0.09^{C}$ | $1.82\pm0.10^{B}$ | $9.36\pm0.53^{B}$ | $38.2\pm0.2^{B}$ |
| Wheat Flour | $1.647\pm0.078^{A}$ | $24.70\pm0.15^{B}$ | $7.53\pm0.32^{A}$ | $3.29\pm0.13^{C}$ | $49.9\pm0.5^{A}$ |
| Wheat Farina | $0.395\pm0.048^{B}$ | $28.37\pm0.41^{A}$ | $1.54\pm0.09^{B}$ | $18.4\pm0.77^{A}$ | $34.0\pm0.1^{C}$ |

The compressibility results followed trends with the cohesion results, with flour being most-compressible, followed by starch, and farina being the least-compressible, as is expected from the explanation provided by Peleg (1971).

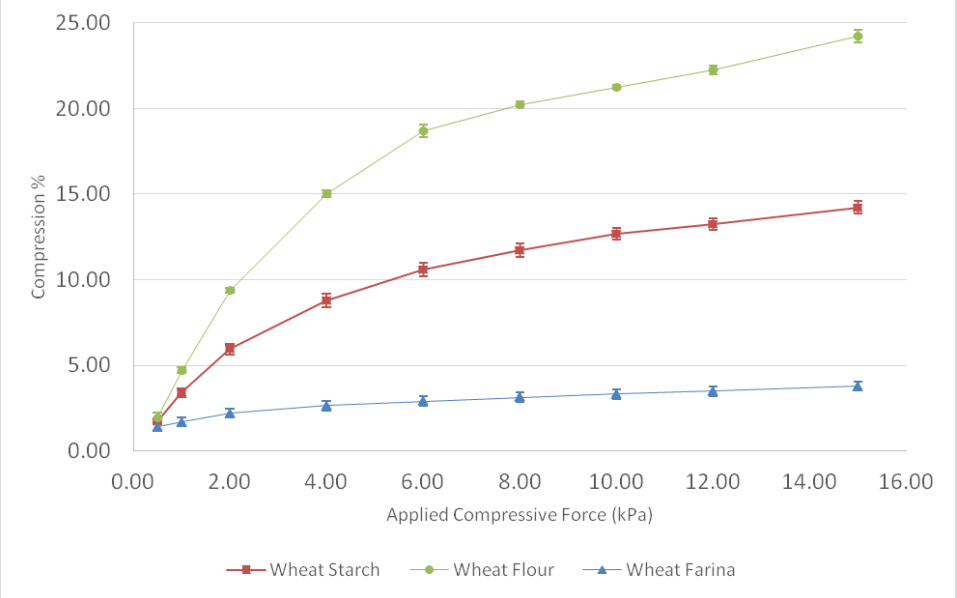


**Figure 2-7 Compressibility Results of Wheat Powders**

Wall friction testing for wheat showed a similar trend as corn—a greater particle size tended to correlate to lower wall friction angle. As the difference in particle size between wheat flour and farina was much less than corn flour and meal, the values for

wheat were much closer in this test. Additional forces, such as interparticle friction or cohesion may play a role in these values as well—a greater internal influence may negate or lessen the effect of external forces applied to a powder.

**Table 2.7 Wall Friction Results of Wheat Powders**

| Sample | WFA |
|---|---|
| Wheat Starch | $17.6 \pm 0.2^{A}$ |
| Wheat Flour | $4.2 \pm 0.3^{C}$ |
| Wheat Farina | $5.6 \pm 0.0^{B}$ |

*2.3.5 Sugar Particle Size*

Sugar, being the only non-starch-based powder tested, showed different results when particle size became large. While powdered and superfine sugar yielded trends in SBFE and SE that followed the pattern of corn and wheat powders, granulated sugar required over four times the energy for both. This could be partly due to the shape of the powder, as powdered sugar and superfine sugar are both more rounded particles, while granulated sugar is longer with asymmetrical edges (Rogé 2000). This shape may cause granules to interlock and create a more difficult matrix for the blade to traverse, in both confined and unconfined flow. While the variation is too great to show clear distinction between SIs, the results indicate greater compacting consolidation as particle size increased. Conversely, as particle size increased, sensitivity to blade tip speed was reduced, denoted by the decreasing FRI value. Powdered sugar was the most sensitive to a ten-fold decrease in blade speed, while superfine sugar was mostly unaffected. Granulated sugar, with a value of <1.0, indicates that a slower blade speed was more

efficient for traversing through the powder. Particle geometry may again explain this, as a slower tip speed may gently disrupt the interlocking particles smoother than the faster blade speed (similar to how non-Newtonian fluids behave as solids when acted upon by high forces, but flow freely when forces below the threshold for behaving as a solid are applied)

**Table 2.8 Stability Results for Sugar Powders**

| Sample | SBFE | SE | SI | FRI |
|---|---|---|---|---|
| Powdered Sugar | $9.30\pm0.12^{C}$ | $9.27\pm0.02^{B}$ | $1.05\pm0.02^{A}$ | $1.72\pm0.00^{A}$ |
| Superfine Sugar | $8.02\pm0.49^{B}$ | $4.17\pm0.49^{C}$ | $1.11\pm0.09^{A}$ | $1.02\pm0.02^{B}$ |
| Granulated Sugar | $51.73\pm5.05^{A}$ | $10.90\pm0.40^{A}$ | $1.07\pm0.03^{A}$ | $0.91\pm0.04^{C}$ |

Additionally, the FF for superfine sugar was the highest of all powders, while powdered sugar was lowest of all, which is confirmed by the cohesion values being the lowest and highest, respectively. Lastly, the AIF(E) follows the expected relation with cohesion, with powdered sugar having the highest angle, followed by granulated sugar, and superfine sugar having the lowest value. The values of granulated and powdered sugars, while lower than reported by Stasiak (2004), display the same pattern.

**Table 2.9 Shear Results for Sugar Powders**

| Sample | Cohesion | MPS | UYS | FF | AIF(E) |
|---|---|---|---|---|---|
| Powdered Sugar | $2.180\pm0.130^{A}$ | $15.10\pm0.15^{B}$ | $10.83\pm0.50^{A}$ | $1.40\pm0.06^{C}$ | $65.9\pm1.0^{A}$ |
| Superfine Sugar | $0.191\pm0.039^{C}$ | $15.13\pm0.03^{B}$ | $0.62\pm0.06^{C}$ | $24.73\pm2.31^{A}$ | $37.8\pm0.3^{C}$ |
| Granulated Sugar | $0.807\pm0.092^{B}$ | $27.17\pm0.93^{A}$ | $3.28\pm0.34^{B}$ | $8.53\pm1.17^{B}$ | $40.5\pm0.4^{B}$ |

Like corn and wheat powders, sugar showed a correlation between cohesion and compressibility. Powdered sugar had the highest cohesion of any of the nine powders tested and was the most compressible, as well. Both superfine and granulated sugars had low cohesion values, which was reflected in a low compressibility (comparatively lower compressibility for superfine than granulated sugar, to match with the comparatively lower cohesion value).

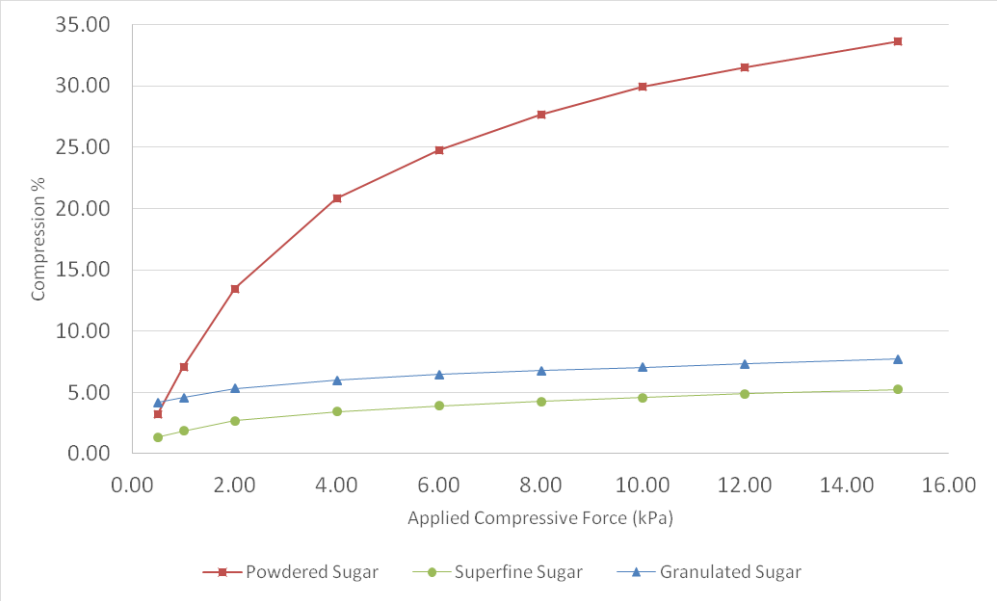


**Figure 2-8 Compressibility of Sugar Powders**

The wall friction testing for sugar powders yielded results that appear to run contrary to the previous corn and wheat powders—while cohesion values had an inverse relationship with wall friction angle of corn and wheat, particle size appeared to have an inverse correlation with wall friction angle for sugar. However, like the results of SBFE/SE, the particle geometry may give skewed results. While particles may not have been able to intermesh during the dynamic testing with the shearing blades constantly rotating during the shear test, the wall friction test had no such disruptions to the particle matrix and simply tested surface interactions after compression.

**Table 2.10 Wall Friction Results for Sugar Powders**

| Sample | WFA |
|---|---|
| Powdered Sugar | $26.8\pm1.0^{A}$ |
| Superfine Sugar | $12.8\pm0.5^{B}$ |
| Granulated Sugar | $9.5\pm0.2^{C}$ |

*2.3.6 Fine Particle Size*

As the composition varies between each powder, no trends are immediately visible. However, the starch-based powders do show a lesser resistance when blade speed was changed for FRI testing. Each powder appeared to show a different behavior than the others—powdered sugar and, to a lesser extent, corn starch, appeared to be unimpacted by confined versus unconfined flow, yet wheat starch showed a substantial decrease from confined to unconfined flow energy. While all powders compacted during conditioning, corn starch appeared to be the least stable, with the highest value for SI, while wheat starch and powdered sugar were both closer to an index value of 1.

**Table 2.11 Stability Results for Fine Powders**

| Sample | SBFE | SE | SI | FRI |
|---|---|---|---|---|
| Corn Starch | $11.01\pm0.08^{B}$ | $12.93\pm0.69^{A}$ | $1.18\pm0.03^{A}$ | $1.61\pm0.04^{B}$ |
| Wheat Starch | $14.24\pm0.11^{A}$ | $8.64\pm0.26^{B}$ | $1.07\pm0.03^{B}$ | $1.63\pm0.01^{B}$ |
| Powdered Sugar | $9.30\pm0.12^{C}$ | $9.27\pm0.02^{B}$ | $1.05\pm0.02^{B}$ | $1.72\pm0.00^{A}$ |

As previously mentioned, the FF values in this study are greater than visually-expected results for starch products. However, the AIF(E) is similar to, and follows the trend of, research done by Stasiak et al. which reported AIF(E) for corn and wheat starches at 38 and 42 degrees, respectively (2013). However, the trend of cohesion

relating to AIF(E) is still present, as powdered sugar has an AIF(E) value nearly double that of the starch powders.

**Table 2.12 Shear Results for Fine Powders**

| Sample | Cohesion | MPS | UYS | FF | AIF(E) |
|---|---|---|---|---|---|
| Corn Starch | $0.440\pm0.099^{B}$ | $23.20\pm0.15^{A}$ | $1.93\pm0.04^{B}$ | $12.03\pm0.26^{A}$ | $34.1\pm0.2^{C}$ |
| Wheat Starch | $0.468\pm0.029^{B}$ | $16.93\pm0.09^{B}$ | $1.82\pm0.10^{B}$ | $9.36\pm0.54^{B}$ | $38.2\pm0.2^{B}$ |
| Powdered Sugar | $2.180\pm0.130^{A}$ | $15.10\pm0.15^{C}$ | $10.83\pm0.50^{A}$ | $1.40\pm0.06^{C}$ | $65.9\pm1.0^{A}$ |

Cohesion results correlated extremely well with the compressibility data. Corn starch is only slightly less compressible than wheat starch, while the two have cohesion values that are not statistically different. In contrast, powdered sugar was drastically more compressible and had a cohesion value substantially higher than the two starch powders.

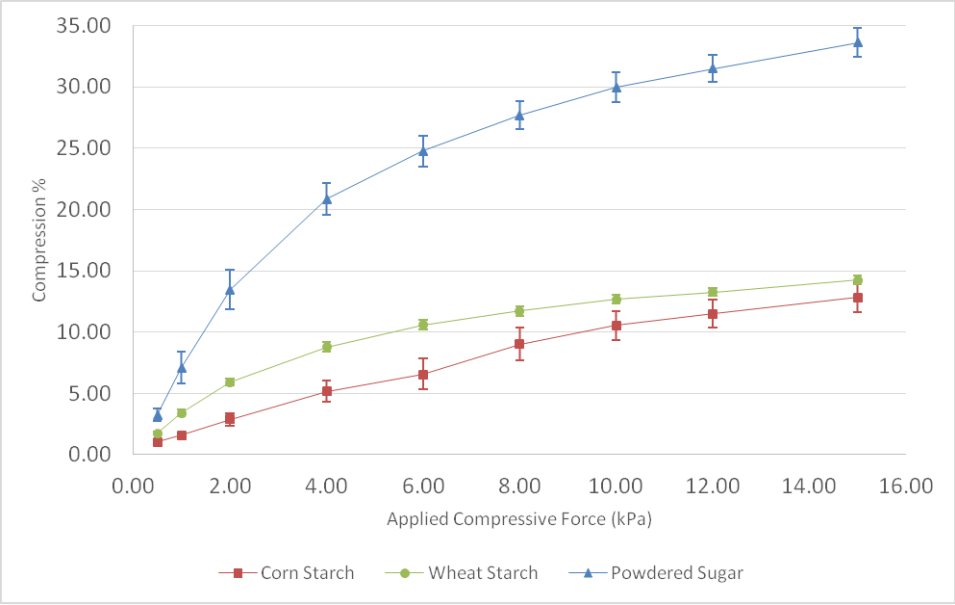


**Figure 2-9 Compressibility of Fine Powders**

In contrast to previous sections, where cohesion appeared to play a role in wall friction angles, the opposite appears to be true when comparing similar particle size powders of different compositions. The correlation with comparing cohesion results to wall friction results may not be concrete, however, and starch-based food powders may simply interact more internally and less with wall surfaces than sucrose-based food powders.

**Table 2.13 Wall Friction Results for Fine Powders**

| Sample | WFA |
|---|---|
| Corn Starch | $13.1\pm0.5^{C}$ |
| Wheat Starch | $17.6\pm0.2^{B}$ |
| Powdered Sugar | $26.8\pm1.0^{A}$ |

*2.3.7 Medium Particle Size*

Corn flour has the undisputed highest energy requirements during both confined and unconfined flow, while wheat flour and superfine sugar overlapped in confined flow energy requirements, starch-based powders required more energy in unconfined flow than sugar.

**Table 2.14 Stability Results for Medium Powders**

| Sample | SBFE | SE | SI | FRI |
|---|---|---|---|---|
| Corn Flour | $10.71\pm0.05^{A}$ | $8.36\pm0.05^{A}$ | $1.07\pm0.04^{A}$ | $1.38\pm0.01^{A}$ |
| Wheat Flour | $7.94\pm0.08^{B}$ | $6.50\pm0.85^{A}$ | $1.12\pm0.03^{A}$ | $1.21\pm0.01^{B}$ |
| Superfine Sugar | $8.02\pm0.05^{B}$ | $4.17\pm0.50^{B}$ | $1.11\pm0.09^{A}$ | $1.02\pm0.02^{C}$ |

Starch-based powders showed a definitively higher cohesion value, leading to lower FF and higher AIF(E) than superfine sugar. These results also correlated to

superfine sugar being substantially less compressible than both of the flours. Additionally, the slightly higher cohesion value of corn flour when compared to wheat flour resulted in corn flour being slightly more compressible than wheat flour, clearly showing a strong correlation between the two values—cohesion and compressibility. AIF(E) of corn flour was drastically higher than previous studies (Alavi and Ambrose, 2015) but Cohesion and FF values of the material were extremely similar, and yielded similar trends during the inline validation study performed in Chapter 5.

**Table 2.15 Shear Results for Medium Powders**

| Sample | Cohesion | MPS | UYS | FF | AIF(E) |
|---|---|---|---|---|---|
| Corn Flour | $1.797\pm0.073^{A}$ | $20.43\pm0.09^{A}$ | $8.67\pm0.30^{A}$ | $2.36\pm0.07^{B}$ | $58.5\pm0.3^{A}$ |
| Wheat Flour | $1.647\pm0.079^{A}$ | $24.70\pm0.15^{B}$ | $7.53\pm0.32^{B}$ | $3.29\pm0.13^{B}$ | $49.9\pm0.5^{B}$ |
| Superfine Sugar | $0.191\pm0.039^{B}$ | $15.13\pm0.03^{C}$ | $0.62\pm0.06^{C}$ | $24.73\pm2.31^{A}$ | $37.8\pm0.3^{C}$ |

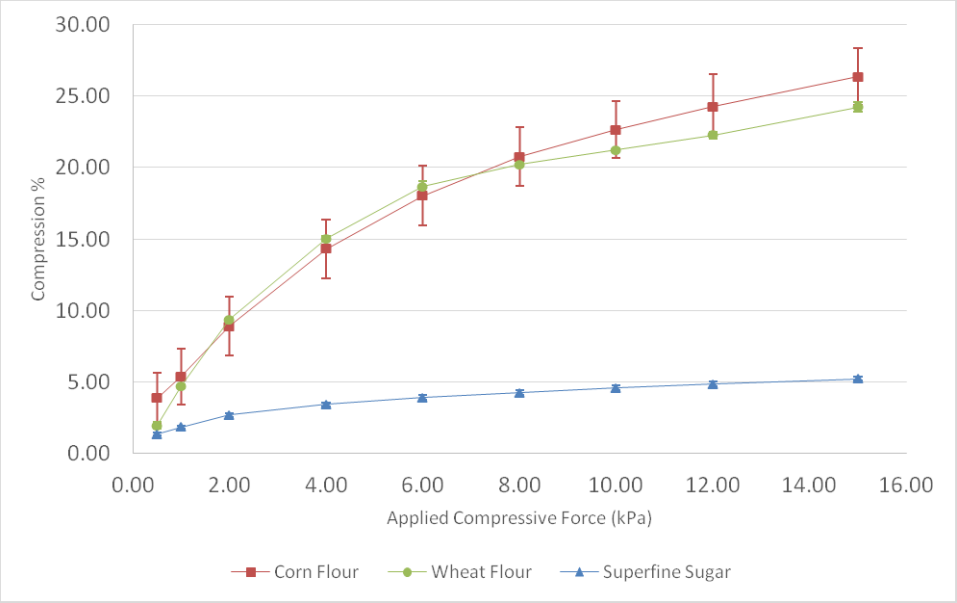


**Figure 2-10 Compressibility of Medium Powders**

Similar to results of fine particles, starch-based powders yielded a lower wall friction angle, indicating that even with slightly increased particle size, sucrose-based powders interact more strongly with surfaces than starch-based powders do. While composition most likely plays a large role in this, particle shape may be a factor, as well.

**Table 2.16 Wall Friction Results for Medium Powders**

| Sample | WFA |
|---|---|
| Corn Flour | $7.7 \pm 0.2^{B}$ |
| Wheat Flour | $4.2 \pm 0.3^{C}$ |
| Superfine Sugar | $12.8 \pm 0.5^{A}$ |

*2.3.8 Coarse Particle Size*

As mentioned previously, the shape of particles appeared to play a role in inflating the energy required for granulated sugar during both confined and unconfined flow—elaborate. The stability of coarse, starch-based powders indicates that they tend to expand during conditioning while the sucrose-based powder tended to compact. However, due to shape rather than composition, granulated sugar and wheat farina were both less sensitive to a change in blade speed while corn meal was more impacted by the tenfold speed change.

**Table 2.17 Stability Results for Coarse Powders**

| Sample | SBFE | SE | SI | FRI |
|---|---|---|---|---|
| Corn Meal | $6.70 \pm 0.00^{B}$ | $3.77 \pm 0.06^{B}$ | $0.97 \pm 0.01^{B}$ | $1.40 \pm 0.02^{A}$ |
| Wheat Farina | $5.81 \pm 0.09^{B}$ | $2.66 \pm 0.05^{C}$ | $1.00 \pm 0.00^{B}$ | $0.95 \pm 0.01^{B}$ |
| Granulated Sugar | $51.73 \pm 5.05^{A}$ | $10.9 \pm 0.40^{A}$ | $1.07 \pm 0.03^{A}$ | $0.91 \pm 0.04^{B}$ |

Similar to FRI results, corn meal had a noticeably higher cohesion value than wheat farina, similar to that of granulated sugar. Having the highest AIF(E) coupled with the Cohesion values led to corn meal having the lowest FF of the three samples, although still qualifying as a free-flowing powder based on its value.

**Table 2.18 Shear Results for Coarse Powders**

| Sample | Cohesion | MPS | UYS | FF | AIF(E) |
|---|---|---|---|---|---|
| Corn Meal | $0.843\pm0.051^{A}$ | $19.73\pm0.09^{B}$ | $4.02\pm0.22^{A}$ | $4.94\pm0.27^{C}$ | $49.0\pm0.1^{A}$ |
| Wheat Farina | $0.395\pm0.048^{B}$ | $28.37\pm0.41^{A}$ | $1.54\pm0.09^{B}$ | $18.47\pm0.77^{A}$ | $34.0\pm0.1^{C}$ |
| Granulated Sugar | $0.807\pm0.092^{A}$ | $27.17\pm0.93^{A}$ | $3.28\pm0.34^{A}$ | $8.53\pm1.17^{B}$ | $40.5\pm0.4^{B}$ |

From compressibility results, a correlation can be seen between cohesion and an increased compressibility. This indicates that, when composition is the only factor, compressibility can be correlated to cohesion, especially at higher forces. These results are congruent with Molenda et al. where corn meal, soybean meal, and wheat were compressed and changes in bulk densities were recorded (2002)

This is useful information at the front end of a system, when the material is loaded into a feeding hopper. If the hopper is loaded more, a more cohesive product (like corn meal) will compact more and, depending on the feeding mechanism—volumetric or gravimetric—taking care to keep a similar level of compressive force at the bottom of the feeder will become more important. A feeder with 2kPa force at the bottom will have ~3% compression of corn meal (~3% more product in a given volume) whereas 15kPa force will results in a nearly 8% compression (~9% more product in a given volume). If the feeder is volumetric, this will result in a larger consumption of raw material at the

beginning of the system and filling the extruder barrel more than anticipated, which could lead to choking.

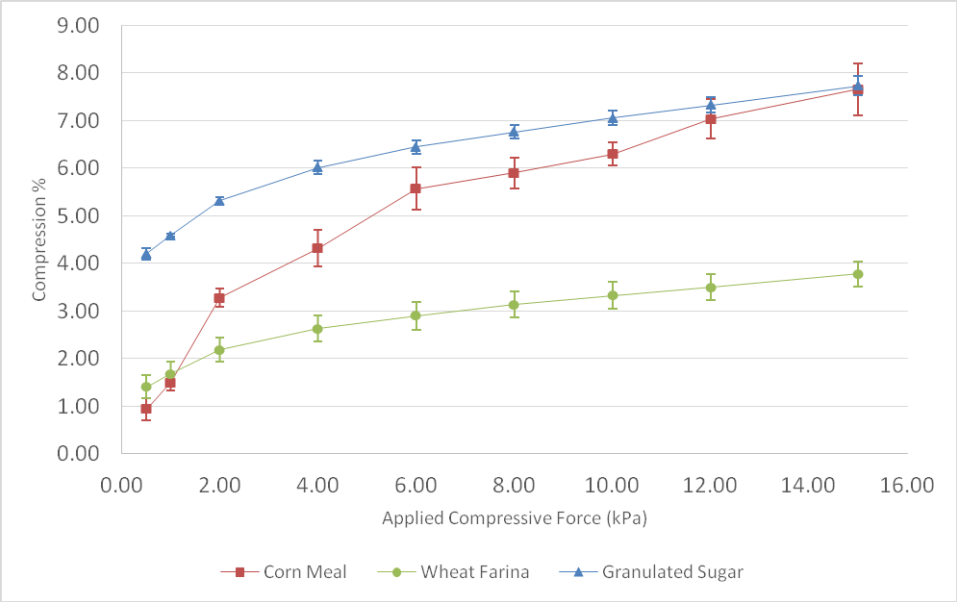


**Figure 2-11 Compressibility of Coarse Products**

Following the trends of fine- and medium-sized particles, starch-based powders demonstrated a lesser wall friction angle than sucrose-based powders. This trend appears to confirm that composition plays a greater role in wall friction angle than strictly correlating results from cohesion without considering composition.

**Table 2.19 Wall Friction Results for Coarse Powders**

| Sample | WFA |
|---|---|
| Corn Meal | $5.8\pm0.1^{B}$ |
| Wheat Farina | $5.6\pm0.0^{B}$ |
| Granulated Sugar | $9.5\pm0.2^{A}$ |

## 2.4 Conclusion

For starch-based powders, energy per unit mass tends to decrease as particle size increases. The larger particles also flow more readily, which makes them ideal for systems such as extruders where energy efficiency of a continuous system is of great value. While granulated sugar was shown to be much higher in energy consumption in confined and unconfined flow, this experiment was run at ambient moisture content, which is not a parameter that extruders operate at, and will be discussed in the following chapter.

As extruder barrels completely encase the food powders, wall friction values are important to note. This value would also pertain to the screw, which could indicate how much slip is present in the extrusion process and, thus, the efficiency of the screw to move different powders from the beginning of the barrel through to subsequent zones in the barrel.

The stability and flow rate indices illustrate the impact that changing the screw speed would have on these food powders, as well as the impact of using a gravimetric feed system into the process—with powders that have an index smaller or larger than 1 (essentially every powder here, to varying degree of severity), volume will change to be greater or lesser, respectively, than the initial volume, and could lead to under- or over-feeding the extruder.

Cohesion results, in tandem with SBFE and FF results provide an insight to the workings of the extruder's feeding zone, as understanding a powder's tendency to resist flow (or flow more readily than anticipated, as could be the case with corn starch) allow for proactive modifications to be made to a system—increasing or reducing screw speed

at start-up (or throughout the entire process) to ensure material is sufficiently conveyed forward, or adding water to reduce the intensity of interparticle forces to aid in forward conveying are just some of the potential solutions to increasing flow properties of the food powders explored here.

In the following chapter, the coarse food powders were subjected to changes in moisture to characterize the impact this modification has on granular flow of material after passing through the preconditioning step, and the subsequent implications these changes have on the extrusion system.

# Chapter 3 - Flow Properties of Coarse Food Powders as a Function of Moisture Content


## Abstract

Extrusion processing relies heavily on the usage of water for aiding in flow and proper processing. If a material is too dry, the high temperature and pressure will cause the material to cook too rapidly and fail to exit the die. If a material is too wet, it will not achieve high enough temperatures to expand upon exiting the die. In order to balance the amount of water introduced in the extruder barrel, extrusion utilizes a preconditioner to add water and steam to the dry material before entering into the actual extruder barrel. Temperatures exiting the preconditioner downspout may be as high as 95°C, and moisture content may be as high as 20%. This chapter focuses on the impact of the latter—using a relative humidity chamber, moisture content of coarse food powders used in the previous chapter (corn, wheat, sugar) was increased to test impact during offline testing with a powder rheometer. Corn meal exhibited an increase in energy requirements as moisture content increased (6.70mJ/g at 13.13% to 9.14mJ/g at 19.61%) but no statistical change in flow functionality ratings (4.94 to 5.11); wheat farina also showed an increase in energy requirement as moisture increased (5.81mJ/g at 13.73% to 9.47mJ/g 19.57%) but a marked decrease in flow functionality ratings (18.47 to 6.1); granulated sugar showed a decrease in energy requirements as moisture increased (51.73mJ/g at 0.06% moisture content to 13.58mJ/g at 0.78% moisture content) and a decrease in flow functionality ratings (8.53 to 3.47).

## 3.1 Introduction

In extrusion processing, material starts in a hopper, is fed through a feeder screw, through a preconditioning system and finally into the extruder for processing. All of this flow takes place as a granular material; it is not until the material enters the kneading and cooking zones that it under goes pressures and temperatures changes that begin to transition the powder into a fluidized mass before exiting the die at the end of the barrel. While this is a simplified illustration of an extrusion system, and each target product has different optimal processing parameters—moisture added, thermal energy added, screw profile, barrel temperature, et al.—the zones, and physiochemical changes that occur in said zones, are always present.

As mentioned in the previous chapter, particle size, shape, and general composition are all important to determine flow functionality of granular material. However, some products such as pet food or other high-protein products require conditioning prior to entering the feeding zone of the extruder. By using a preconditioner, thermal energy (in the form of steam) and moisture (in the form of water) can be added to the raw material, partially cooking it or to achieve processing parameters during extrusion (increasing moisture content to aid in cooking or to reduce mechanical shear, for example). The increased moisture content modifies the surface chemistry of the still-granular material, resulting in agglomeration that can lead to clumping or further resistance to flow, depending on the composition of the powder and how this surface moisture impacts the granules. Stoklosa et al. (2012) found significant impact of relative humidity and formulation on powder flowability, which indicated that physical and chemical changes on the surface of material due to increased moisture in the air plays a

critical role in increasing angle of internal friction and reducing flow properties. Differences in physical and chemical properties of particles vary from one compound to another and affect the cohesive forces acting between particles and capillary forces associated with liquid bridging (Fitzpatrick et al. 2004). Increased powder strength as a result of absorption of moisture from the atmosphere has been researched since the 1960s, due to the problems in regards to flow and other process-related issues this phenomenon causes (Rabinovich et al. 2005).

### *3.1.1 Objectives*

1. Explore correlation of flow properties, energy requirements as moisture content of coarse food powders increases

## 3.2 Materials and Methods

### *3.2.1 Materials*

The materials used for this experiment were as follows: Corn meal (Aunt Jemima, Chicago, IL), wheat farina (Hal Ross Mill, Kansas State University, Manhattan, KS), and granulated sugar (C&H, Yonkers, NY).

### *3.2.2 Moisture Modification*

To increase the moisture content of each material, a relative humidity chamber was used. Corn meal and farina were placed in the chamber at 22°C and 95% Relative Humidity for 2 hours (to achieve mid-range moisture content) or 4 hours (to achieve high-range moisture content). Granulated sugar was placed in the chamber at 22°C and 85% Relative Humidity for 3 hours (to achieve mid-range moisture content) or 4 hours (to achieve high-range moisture content).

### *3.2.3 Moisture Testing*

AOAC Moisture Method 930.15 was employed for all samples, in triplicate, to ascertain initial moisture content using a conventional drying oven at 135°C for 2 hours.

### *3.2.4 Equipment and Testing Methods*

The Freeman Technology FT4 Powder Rheometer was used to perform four powder property tests: Stability and Variable Flow Rate, Compressibility, Shear Cell, and Wall Friction. These tests have been outlined previously. See Chapter 2, Section 2.2.4 for equations and visual aids

#### *3.2.4.1 Stability and Variable Flow Rate*

Basic Flowability Energy (BFE) is the total energy used for the blade traverse to downwards in the seventh cycle of the testing process, which represents confined flow (as the blade moved toward the base of the sample, meeting resistance). The higher this value, the more energy required for this cycle

Specific Basic Flow Energy (SBFE) is BFE divided by total mass of product in the cylinder to give Joules/gram, which allows for a more uniform comparison across products with different densities, as formulations for products are mixed on a per-mass basis, not per-volume basis.

In contrast to BFE, Specific Energy (SE) represents the energy taken to move from the base of the cylinder to the top, representing unconfined flow.

Stability Index shows whether a powder expands, compacts, or remains at the same volume through the test cycles. A value near 1.00 indicated the powder maintains its volume, while a value greater or less than 1.00 indicated the powder had a tendency to compact or expand, respectively

Finally, Flow Rate Index (FRI) is the factor by which flow energy is changed when the blade tip speed is reduced by a factor of 10. It evaluates the sensitivity of the powder to different flow rates.

*3.2.4.2 Compressibility*

After the conditioning cycle was completed, the blade was replaced by a 48mm-diameter vented piston. The top cylinder was split to remove excess powder, leaving a standard volume of product, and then the piston was lowered at increasing force levels and the percentage compression of the powder was recorded. These force/compression results were plotted on a graph internally and presented at the completion of the test

*3.2.4.3 Shear Cell*

Testing of shear properties allows for further understanding of inter-particulate forces powders are subjected to during handling and processing, such as the yield point of powder flow initiation. Preparation for the Shear Cell test involved using the 48mm helical blade, followed by the 48mm diameter vented piston, and then splitting the two 85mm x 50mm glass cylinders, leaving a compacted volume of sample for the test. The shear cell attachment, with the same radius as the vented piston but with small blades on the underside, was used to carry out the test by inducing rotational and vertical stress. Once the powder bed in the cylinder yielded to the stress applied by the shear head, the stress value was recorded.

These results utilized the Mohr Circle analysis to calculate values such as cohesion, Major Principle Stress, Unconfined Yield Strength, and Flow Factor.

For further explanation on Mohr Circles, plotting/analysis of the aforementioned values, and Flow Function ratings, see section 2.2.4.3 in the previous chapter.

*3.2.4.4 Wall Friction*

This test measures the resistance of flow of powders in relation to the process equipment surface by using a friction disc head that applies both vertical and rotational stress on a powder at rest to determine the torque necessary to overcome the resistance of the powder bed. A Wall Friction disc, with a μ-value of 0.05, was used for the test. The torque required to maintain the rotational momentum of the disc was measured and used to calculate a 'steady-state' shear stress. The normal stress was maintained constant throughout the measurement.

## 3.3 Results and Discussion

*3.3.1 Moisture Content*

Moisture content for corn meal was determined to be 13.13% (ambient), 15.46% (mid-range), and 19.61% (high); wheat farina was determined to be 13.73% (ambient), 15.69% (mid-range), and 19.57% (high); granulated sugar was determined to be 0.06% (ambient), 0.40% (mid-range), and 0.78% (high).

*3.3.2 Corn Meal*

As moisture content increased for corn meal, the energy per gram required consistently increased for confined flow parameters. For unconfined flow, the trend appears to show that energy requirements are also increased, although the values are all fairly similar. The same is true for the Stability Index—an increase in moisture content appears to yield a higher Stability Index value, although the values are somewhat similar. Regardless, moisture increases clearly show stability results greater than one, unlike the initial moisture sample. Lastly, Flow Rate Index shows that, as moisture increases, the sensitivity to blade speed is reduced, denoted by the value gradually moving closer to

1.00. While the initial energy requirement is higher than the lower moisture content, a reduced blade speed required less additional energy at higher moisture contents.

**Table 3.1 Stability Results for Corn Meal, Moisture**

| Corn Meal Sample | S.BFE | SE | SI | FRI |
|---|---|---|---|---|
| 13.13% MC | $6.70\pm0.00^{C}$ | $3.77\pm0.06^{A}$ | $0.97\pm0.01^{B}$ | $1.40\pm0.02^{A}$ |
| 15.45% MC | $8.32\pm0.04^{B}$ | $4.21\pm0.06^{B}$ | $1.15\pm0.06^{A}$ | $1.27\pm0.02^{B}$ |
| 19.61% MC | $9.14\pm0.03^{A}$ | $4.31\pm0.03^{B}$ | $1.05\pm0.03^{AB}$ | $1.14\pm0.00^{C}$ |

The results from the shear testing appear counterintuitive to patterns that were established in the previous chapter—even though cohesion tended to increase, the effective angle of internal friction clearly decreased, indicating that there was no longer a clear relationship between these two values. Additionally, the flow factor tended to increase as well. Combining all this information, it can be inferred that corn meal agglomerates as moisture content increases, but would be intrinsically inclined to move as an agglomerated mass as opposed to having a propensity for remaining stationary as a cohesive mass. Downton et al (1982) reported a model that suggests when two moistened particles come into contact, they build a bridge with sufficient strength to overcome mechanical deformation and increasing cohesive forces. While cohesion of corn meal did not substantially increase, the irregular particle shape may have been of greater consequence than the model described by Downton.

**Table 3.2 Shear Results for Corn Meal, Moisture**

| Corn Meal Sample | Cohesion | MPS | UYS | FF | AIF(E) |
|---|---|---|---|---|---|
| 13.13% MC | $0.843\pm0.088^{A}$ | $19.73\pm0.08^{B}$ | $4.02\pm0.22^{A}$ | $4.94\pm0.27^{A}$ | $49.0\pm0.1^{A}$ |
| 15.45% MC | $0.903\pm0.081^{A}$ | $20.90\pm0.15^{A}$ | $4.09\pm0.21^{A}$ | $5.15\pm0.32^{A}$ | $46.5\pm0.4^{B}$ |
| 19.61% MC | $0.951\pm0.036^{A}$ | $18.87\pm0.18^{C}$ | $3.70\pm0.15^{A}$ | $5.11\pm0.16^{A}$ | $42.4\pm0.1^{C}$ |

The compressibility results do mirror the cohesion results from the shear testing, although there is a more drastic difference between initial compressibility and samples with additional moisture. Here, it can be seen that the addition of moisture definitively increases compressibility, although increasing the moisture content further appears to have a drastically mitigated effect. This correlation makes sense, as the increase in cohesion values would result in granules of corn meal sticking more readily, causing more void space between particles even after the conditioning cycle of the test and, in turn, allowing more opportunity for compressibility as these void spaces are filled with corn meal particles.

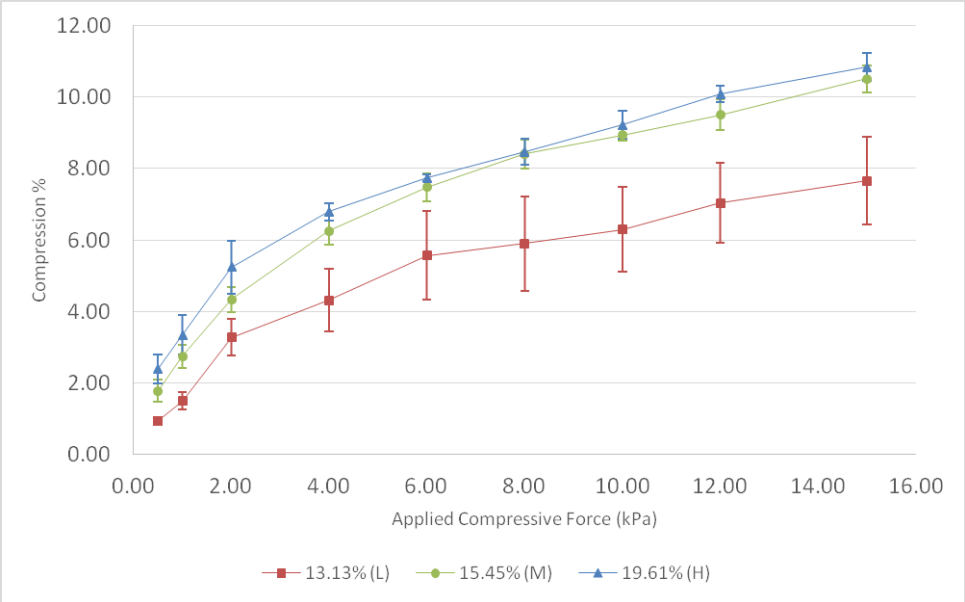


**Figure 3-1 Compressibility of Corn Meal, Moisture**

Despite having a slightly increased flow factor, an increase in moisture of corn meal resulted in a significant increase in wall friction interaction, with greater moisture content yielding a greater surface-wall interactive force.

**Table 3.3 Wall Friction Results for Corn Meal, Moisture**

| Corn Meal Sample | WFA |
|---|---|
| 13.13% MC | $5.8\pm0.1^{A}$ |
| 15.45% MC | $8.4\pm0.5^{B}$ |
| 19.61% MC | $10.5\pm0.1^{C}$ |

Based on these results, it would appear that an increase in moisture content (to the ranges utilized in extrusion preconditioning) impacts the results of the testing performed above. Combining the trends of increased cohesion and flow factor with the decreased angle of internal friction, increased wall friction angle, and increased basic flow energy requirements makes the impact of moisture on flow in an extruder difficult to ascertain, due to the mixing of characteristics that increase flow with those that decrease flow. With the number of traits that appear to increase flow properties, however, it is likely that corn meal would flow as a free or loosely-agglomerated powder when fed into an extruder barrel after preconditioning increases the moisture content.

### *3.3.3 Wheat Farina*

Although slightly less impacted by moisture content than corn meal in some regards, wheat farina shows a definitive increase in energy requirements for confined flow but only a slight tendency of increasing energy during unconfined flow. The stability index also decreased as moisture content increased, which could be a result of the water-soluble starch leeching out and creating a sticky surface for the particles. This sticky surface could cause adhesion with less surface contact, resulting in the powder taking up more volume as the blade cycled through it during testing. This surface chemistry will be important in further analysis in this section, as well.

**Table 3.4 Stability Results for Wheat Farina, Moisture**

| Farina Sample | S.BFE | SE | SI | FRI |
|---|---|---|---|---|
| 13.73% MC | $5.81\pm0.09^{A}$ | $2.46\pm0.08^{A}$ | $1.00\pm0.00^{A}$ | $0.95\pm0.00^{B}$ |
| 15.69% MC | $8.61\pm0.11^{B}$ | $2.74\pm0.18^{A}$ | $0.94\pm0.01^{B}$ | $1.09\pm0.02^{A}$ |
| 19.57% MC | $9.47\pm0.35^{C}$ | $2.81\pm0.15^{A}$ | $0.92\pm0.02^{B}$ | $0.87\pm0.01^{C}$ |

While the initial increase in moisture content appears to have no effect on cohesion and yield strength, there is a substantial decrease in flow function and increase in angle of internal friction. Further increasing the moisture was seen to result in much stronger cohesion results and a higher yield strength, as well as reducing the flow factor. As mentioned previously, one possible reason for these results is the starchy particles adhering in the presence of surface moisture, causing a sticky product that resists flow. Another reason could be due to the partial hydration of the gluten matrix, allowing particles to create a protein matrix on the surface, resisting the greater flowability seen when no additional moisture is added to the system.

**Table 3.5 Shear Results for Wheat Farina, Moisture**

| Farina Sample | Cohesion | MPS | UYS | FF | AIF(E) |
|---|---|---|---|---|---|
| 13.73% MC | $0.395\pm0.048^{B}$ | $28.37\pm0.41^{A}$ | $1.54\pm0.09^{B}$ | $18.47\pm0.77^{A}$ | $34.0\pm0.1^{B}$ |
| 15.69% MC | $0.385\pm0.021^{B}$ | $17.23\pm0.12^{B}$ | $1.61\pm0.05^{B}$ | $10.74\pm0.25^{B}$ | $40.6\pm1.8^{A}$ |
| 19.57% MC | $0.688\pm0.091^{A}$ | $17.77\pm0.20^{B}$ | $2.94\pm0.23^{A}$ | $6.11\pm0.39^{C}$ | $42.4\pm0.5^{A}$ |

The increase of moisture shows a trend of decreased compression. Due to the sticky nature of the particle surface and the matrix that may have been forming across the surfaces, the subsequent decrease in Stability Index (indicating expansion), and increase in cohesive properties, these results make sense despite initially seeming counterintuitive.

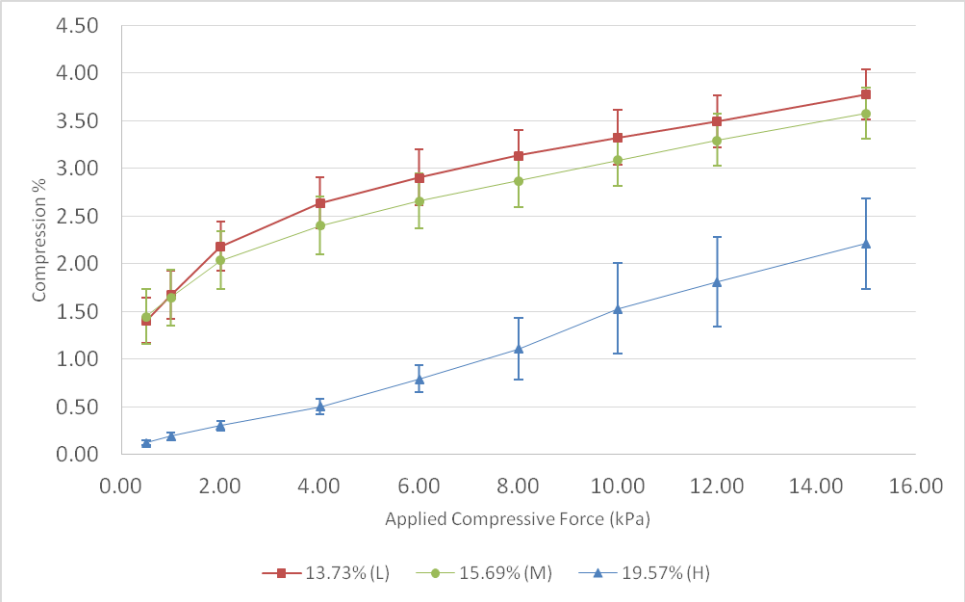


**Figure 3-2 Compressibility of Wheat Farina, Moisture**

As with corn meal, an increase in moisture of wheat farina resulted in increased interaction with surfaces, as shown by the increase in wall friction angle. These interactions would tend to decrease flow in an enclosed environment.

**Table 3.6 Wall Friction Results for Wheat Farina, Moisture**

| Farina Sample | WFA |
|---|---|
| 13.73% MC | $5.6\pm0.0^{C}$ |
| 15.69% MC | $7.9\pm0.3^{B}$ |
| 19.57% MC | $10.0\pm0.1^{A}$ |

The results of moisture addition to wheat farina are easier to draw conclusions from than corn meal in the previous section—increased energy requirements in confined flow, decreased flow factors, increased angles of internal friction, and increased wall friction angles all would lend to a decreased propensity to flow in an extrusion system after exiting the preconditioning system.

The major difference between these starch-based powders appears to be how the materials behave in the presence of moisture. Two primary interactions determine the flow of a powder in a confined space—particle-particle forces and particle-surface forces. Stronger particle-particle forces would increase agglomeration but not necessarily decrease flow properties, as seen by the flow factor of corn meal tending to increase with moisture content. Conversely, stronger particle-surface interactions would decrease flow. As farina has a flow factor that is greatly reduced as moisture increases, the particle-surface interaction (inferred from wall friction results) is more likely to create a poorly-flowing product in tandem with the reduced internal flow characteristics.

### *3.3.4 Granulated Sugar*

Granulated sugar, being the only non-starch powder analyzed within this chapter, behaved much differently than the previous food powders. As moisture content increased (on a much lesser scale, due to the soluble nature of sugar in water), energy requirements decreased for both confined and unconfined flow. The increased flow rate index indicated that moisture content caused a greater sensitivity to the reduced blade speed, despite the overall lesser energy requirements. The stability index remaining relatively constant shows that the sugar does not readily compact more during conditioning/testing cycles due to increased surface moisture.

**Table 3.7 Stability Results for Granulated Sugar, Moisture**

| Sugar Sample | S.BFE | SE | SI | FRI |
|---|---|---|---|---|
| 0.06% MC | $51.73\pm5.05^{A}$ | $10.90\pm0.40^{A}$ | $1.07\pm0.03^{A}$ | $0.91\pm0.04^{B}$ |
| 0.40% MC | $14.72\pm0.61^{B}$ | $8.60\pm0.06^{B}$ | $1.08\pm0.02^{A}$ | $1.19\pm0.01^{A}$ |
| 0.78% MC | $13.58\pm0.21^{B}$ | $6.94\pm0.32^{C}$ | $1.08\pm0.04^{A}$ | $1.23\pm0.00^{A}$ |

Similar to wheat farina, cohesion values overlap for the first two moisture samples but a decrease in flow factor and increase in angle of internal friction are present; the high-moisture sample clearly shows a cohesive product that has a higher propensity for remaining stationary and stacking up (as implied by the increased angle of internal friction).

**Table 3.8 Shear Results for Granulated Sugar, Moisture**

| Sugar Sample | Cohesion | MPS | UYS | FF | AIF(E) |
|---|---|---|---|---|---|
| 0.06% MC | $0.807 \pm 0.092^{B}$ | $27.17 \pm 0.93^{A}$ | $3.28 \pm 0.34^{A}$ | $8.53 \pm 1.17^{A}$ | $40.5 \pm 0.4^{B}$ |
| 0.40% MC | $0.862 \pm 0.121^{B}$ | $17.70 \pm 0.25^{B}$ | $3.51 \pm 0.47^{A}$ | $5.23 \pm 0.69^{B}$ | $42.6 \pm 0.3^{A}$ |
| 0.78% MC | $1.233 \pm 0.107^{A}$ | $16.57 \pm 0.09^{B}$ | $4.83 \pm 0.36^{A}$ | $3.47 \pm 0.25^{B}$ | $43.5 \pm 0.1^{A}$ |

Compressibility results for granulated sugar resume the correlation with cohesion, unlike wheat farina in the previous section—the first two samples (0.06%, 0.40% moisture content) are nearly identical in compressibility (from 4kPa force and above) while the 0.80% moisture is drastically more compressible. This could also be due to the sample beginning to melt with the high moisture content, exceeding a threshold for maintaining shape and solid form, and resulting in the sample condensing under pressure to eliminate air pockets created due to the shape of the dry, crystalline structure.

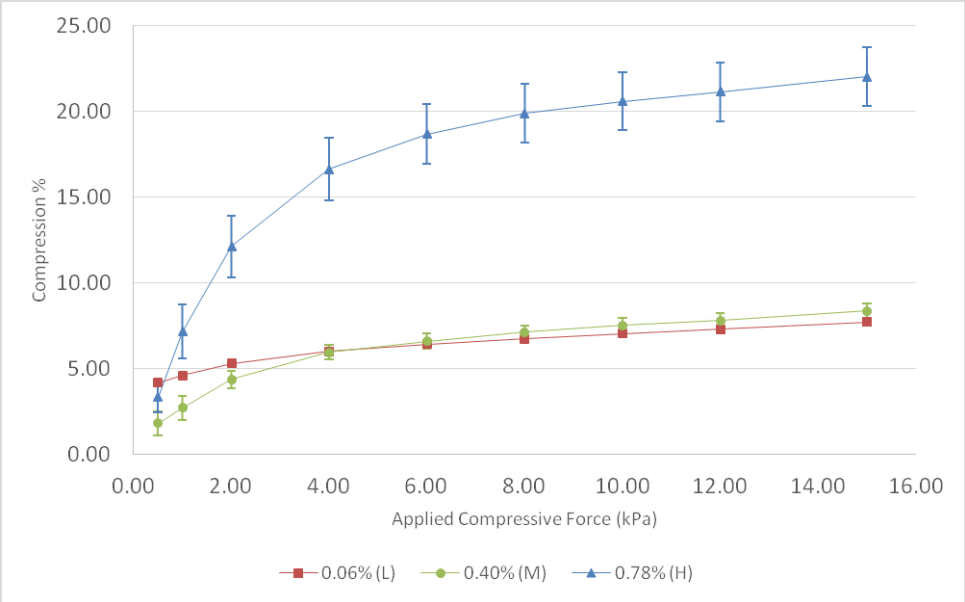


**Figure 3-3 Compressibility of Granulated Sugar, Moisture**

The increase in moisture content decreased particle interactions with walls, shown by the decrease in wall friction angle. Due to the high cohesion and angle of internal friction, the decrease in wall friction angle can be explained due to the interparticle forces increasing with moisture content more than particle-surface interactions.

**Table 3.9 Wall Friction Results for Granulated Sugar, Moisture**

| Sugar Sample | WFA |
|---|---|
| 0.06% MC | $9.5\pm0.2^{A}$ |
| 0.40% MC | $7.9\pm0.0^{B}$ |
| 0.78% MC | $6.3\pm0.0^{C}$ |

## 3.4 Conclusion

While granulated sugar would not be incorporated into systems that use moisture levels this low, the results here show how differently a powder can behave based on its composition when exposed to changes in moisture content. Each of the three powders analyzed in this chapter behaved uniquely when all results were compiled—corn meal became more cohesive but free-flowing and more compressible; farina became less compressible, more cohesive, and less free-flowing; sugar became more cohesive, more compressible, and less free-flowing.

Similar results for corn and wheat powders have been reported prior. Abu-hardan (2010) studied the impact of moisture on wheat and maize starches and flours, finding that caking ability of maize flour was largely uninfluenced by an increase in moisture content while wheat flour showed an enormous increase in cake-forming ability. In addition to the interparticle and particle-wall forces interpreted in this chapter, the difference in caking properties may also be attributed to a partial activation of the gluten matrix in wheat powders, further supporting the correlations found in this experiment.

An in-line flow study, shown in Ch.5, was performed on corn meal and wheat farina, targeting the moisture contents in this chapter to verify flow properties that were inferred from the offline results gathered in this chapter. The results from the in-line study were gathered to develop computer-simulated flow, also discussed there.

# Chapter 4 - Flow Properties of Starch-Based Food Powders as a Function of Temperature


## Abstract

Using an aluminum cylinder wrapped with silicone heating tape to replace the traditional Pyrex® glassware associated with the Freeman Technology FT4 Powder Rheometer, the temperature of corn meal and farina was increased (from 22°C up to 82°C) to discern the difference in flow properties of starch-based materials as a function of temperature. Stability and Variable Flow Rate, Compressibility, Shear, and Wall Friction tests were all performed to show these changes, where farina decreased in energy as temperature increased (14.4mJ/g at 22°C to 12.1mJ/g at 82°C) while corn meal energy requirements increased (12.9mJ/g at 22°C to 17.2mJ/g at 82°C). A decrease in flow functionality was observed for both materials, as well as a tendency to compress more at increased temperatures.


## 4.1 Introduction

From previous chapters, the influence of particle size/shape and composition, as well as moisture content, all have been found to impact flowability of granular material in extrusion systems. In addition to these factors, the addition of steam in the preconditioner (prior to the extruder barrel) provides thermal energy to increase the temperature of the granular material as it exits the downspout into the extruder.

Prior research has explored the influence of temperature on the flowability and caking phenomena of hygroscopic food powders, focusing on sucrose, fructose, and maltodextrin (Wallack and King 1988), as well as sticky point temperatures of fruit

powders (Caparino et al. 2017). More-related to the food powders to be discussed in this chapter, Iqbal and Fitzpatrick compared three varied food powders [wheat flour, tea, and whey] and the impact on wall friction properties when exposed to increased temperatures (2006). While temperatures in this study were substantially higher than the related study, the results did follow the same trend.

Work regarding the heat-induced activation of gluten has been done (Anno 1981), where wheat flour was heated to 85°C for 30 min (or longer, depending on treatment). By testing gluten strength from pH 1-14, it was found that a pH of ~6 was a local peak hardness of gluten, which is the inherent pH of the material (Egan et al. 1981). Corn meal, lacking gluten, is not effected by that sort of physiochemical change but still undergoes changes with increased temperature due to the gelatinization of starches (Burros et al. 1987).

### *4.1.1. Objectives*

1. Explore correlation between flow functionality, energy requirements of coarse starch-based food powders as temperature is increased.

## 4.2 Materials and Methods

### *4.2.1. Materials*

The materials used for this experiment were: corn meal (Aunt Jemima, Chicago, IL), and wheat farina (Hal Ross Mill, Kansas State University, Manhattan, KS).

### *4.2.2 Moisture Testing*

AOAC Moisture Method 930.15 was employed for all samples, in triplicate, to confirm moisture content using a conventional drying oven at 135°C for 2 hours.

### *4.2.3 Equipment and Testing Methods*

The Freeman Technology FT4 Powder Rheometer was used to perform four powder property tests: Stability and Variable Flow Rate, Compressibility, Shear Cell, and Wall Friction.

An aluminum testing cylinder identically matching the glass cylinder dimensions traditionally used with the Powder Rheometer was created in the Kansas State University Physics Shop, so heat could be safely applied to the surface at increasing temperatures.

A ½" diameter silicone heat tape, internally threaded with copper wire, was wrapped around the aluminum cylinder and plugged in to provide thermal heating of the material inside the cylinder. Room temperature was determined to be 22°C, while mid and high temperatures were set at 52°C and 82°C, respectively. A thermometer was placed in the center of the sample to ensure the targeted heating temperature was achieved before each test was initiated. Power was removed from the heat tape before testing commenced, to avoid further heating of the sample throughout the testing process, although the heat tape remained around the cylinder throughout testing.

#### *4.2.3.1 Stability and Variable Flow Rate*

Basic Flowability Energy (BFE) is the total energy used for the blade traverse to downwards in the seventh cycle of the testing process, which represents confined flow (as the blade moved toward the base of the sample, meeting resistance). The higher this value, the more energy required for this cycle

Specific Basic Flow Energy (SBFE) is BFE divided by total mass of product in the cylinder to give Joules/gram, which allows for a more uniform comparison across

products with different densities, as formulations for products are mixed on a per-mass basis, not per-volume basis.

In contrast to BFE, Specific Energy (SE) represents the energy taken to move from the base of the cylinder to the top, representing unconfined flow.

Stability Index shows whether a powder expands, compacts, or remains at the same volume through the test cycles. A value near 1.00 indicated the powder maintains its volume, while a value greater or less than 1.00 indicated the powder had a tendency to compact or expand, respectively

Finally, Flow Rate Index (FRI) is the factor by which flow energy is changed when the blade tip speed is reduced by a factor of 10. It evaluates the sensitivity of the powder to different flow rates.

*4.2.3.2 Compressibility*

After the conditioning cycle was completed, the blade was replaced by a 48mm-diameter vented piston. The top cylinder was split to remove excess powder, leaving a standard volume of product, and then the piston was lowered at increasing force levels and the percentage compression of the powder was recorded. These force/compression results were plotted on a graph internally and presented at the completion of the test

*4.2.3.3. Shear Cell*

Testing of shear properties allows for further understanding of inter-particulate forces powders are subjected to during handling and processing, such as the yield point of powder flow initiation. Preparation for the Shear Cell test involved using the 48mm helical blade, followed by the 48mm diameter vented piston, and then splitting the two 85mm x 50mm glass cylinders, leaving a compacted volume of sample for the test. The

shear cell attachment, with the same radius as the vented piston but with small blades on the underside, was used to carry out the test by inducing rotational and vertical stress. Once the powder bed in the cylinder yielded to the stress applied by the shear head, the stress value was recorded.

These results utilized the Mohr Circle analysis to calculate values such as cohesion, Major Principle Stress, Unconfined Yield Strength, and Flow Factor.

For further explanation on Mohr Circles, plotting/analysis of the aforementioned values, and Flow Function ratings, see section 2.2.4.3 of this paper.

#### *4.2.3.4 Wall Friction*

This test measures the resistance of flow of powders in relation to the process equipment surface by using a friction disc head that applies both vertical and rotational stress on a powder at rest to determine the torque necessary to overcome the resistance of the powder bed. A Wall Friction disc, with a μ-value of 0.05, was used for the test. The torque required to maintain the rotational momentum of the disc was measured and used to calculate a 'steady-state' shear stress. The normal stress was maintained constant throughout the measurement.

## 4.3 Results and Discussion

### *4.3.1 Corn Meal*

Through the stability and variable flow rate testing, an increase in temperature clearly resulted in an increase in energy required for confined flow. The increase in Flow Rate Index as temperature increases shows that the heated material is more resistant to the reduced blade speed, although the Stability Index shows that the powder becomes more stable throughout the performance of the test as the temperature is increased. The

combination of these two results indicate that powder most likely adheres internally and is not prone to settling during disruptions presented during testing.

**Table 4.1 Stability Results for Corn Meal, Temperature**

| Corn Meal | S.BFE | SE | SI | FRI |
|---|---|---|---|---|
| 22°C | $12.91\pm0.06^{C}$ | $4.94\pm0.03^{A}$ | $0.957\pm0.012^{A}$ | $1.11\pm0.01^{C}$ |
| 52°C | $13.99\pm0.06^{B}$ | $5.00\pm0.03^{A}$ | $0.985\pm0.003^{A}$ | $1.37\pm0.02^{A}$ |
| 82°C | $17.20\pm0.09^{A}$ | $4.80\pm0.08^{A}$ | $0.978\pm0.006^{A}$ | $1.21\pm0.02^{B}$ |

The Shear test proved difficult to obtain heat-modified data for—the aluminum cylinder/heating apparatus was not part of the original testing design, so a new baseline was performed separately from the previous chapters. These results took seven or more runs to obtain for each sample, as there were repeatedly errors or faults due to material slippage against the cylinder walls, so the following results were only evaluated on the trends amongst the samples, not the concrete values provided by the testing method. However, despite the challenges in obtaining data, these trends align with results from Wallack and King (1988), which found dry particles exposed to higher temperatures have a diminished flowability.

**Table 4.2 Shear Testing Results for Corn Meal, Temperature**

| Corn Meal | Cohesion | MPS | UYS | FF | AIF(E) |
|---|---|---|---|---|---|
| 22°C | $0.164\pm0.010^{B}$ | $13.87\pm0.15^{B}$ | $0.72\pm0.04^{C}$ | $19.33\pm0.89^{A}$ | $41.7\pm0.1^{B}$ |
| 52°C | $0.279\pm0.040^{B}$ | $16.90\pm1.00^{A}$ | $1.38\pm0.18^{B}$ | $12.63\pm1.82^{B}$ | $47.9\pm0.7^{A}$ |
| 82°C | $0.746\pm0.079^{A}$ | $14.53\pm0.32^{B}$ | $3.06\pm0.25^{A}$ | $4.81\pm0.28^{C}$ | $47.8\pm0.5^{A}$ |

While the initial values differ widely from previous chapters (when comparing the room temperature sample in this chapter with the results in Chapters 2 and 3), it was still

observed that an increase in temperature had a strong increase on cohesion and UYS, which resulted in a decreased Flow Factor. However, the angle of internal friction only appeared to increase beyond room temperature to a point, demonstrated by the medium and high temperatures not being statistically different from each other.

Similar to the angle of internal friction, compressibility results showed two general lines—unheated corn meal compressed the least; both heated samples compressed in a similar range, although there was a much wider range of results for the medium temperature sample. With the increased cohesion and UYS values seen during shear testing, these results generally make sense although, based on previous chapters, corn meal has shown a stronger correlation between compressibility and cohesion so a higher compressibility at 82°C was expected.

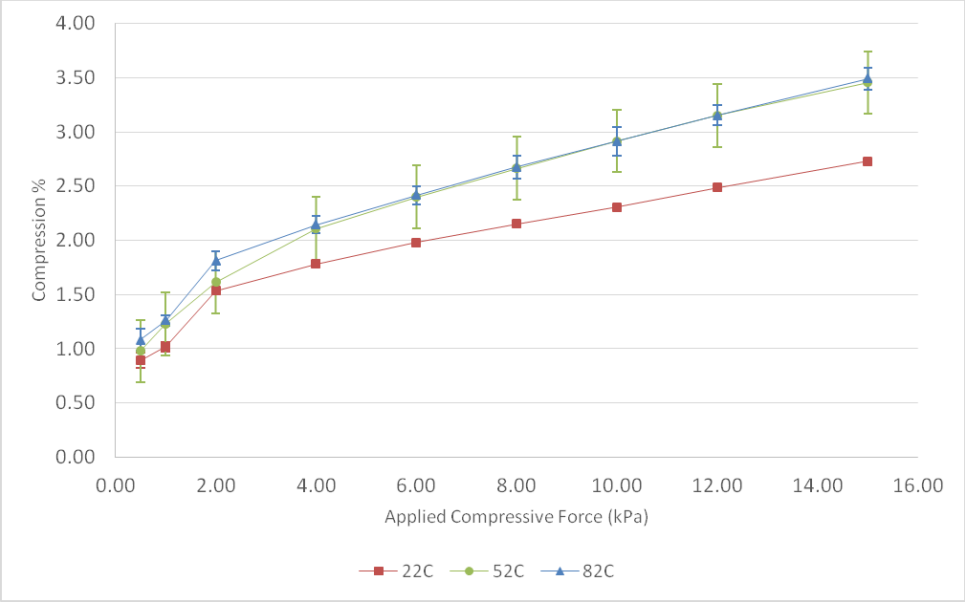


**Figure 4-1 Compressibility Results for Corn Meal, Temperature**

As seen with previous tests in this chapter, the trend from wall friction testing indicated that the wall friction angle tended to increase as temperature increased. While not as drastic of an increase as wheat farina in the following section, the results are not insignificant.

**Table 4.3 Wall Friction Results for Corn Meal, Temperature**

| Corn Meal | WFA |
|---|---|
| 22°C | $6.2\pm0.1^{C}$ |
| 52°C | $8.0\pm0.0^{B}$ |
| 82°C | $9.3\pm0.2^{A}$ |

Overall, these results show that corn meal becomes not only intrinsically more difficult to flow as temperature increases, but also interacts stronger with surfaces as temperature rises. This is most likely due to the starch gelatinization, making the surface slightly sticky and adhering to any available surface—particle or a wall. As extrusion processing involves high temperatures in an enclosed barrel, both of these factors would have an impact on the flow of this powdered material as it enters the extruder barrel.

### *4.3.2 Wheat Farina*

As seen in the previous chapter, wheat farina behaved differently than corn meal when exposed to physical modifications in the form of moisture content. Heat modification was no exception, as farina required less energy for both confined and unconfined flow as the temperature was raised. However, both the stability index and flow rate index increased. The former illustrates that farina compacts more during the trials when heat is applied; the latter indicating that farina becomes more sensitive to

blade tip speed as temperature increases, tending to require more energy at slower blade speeds as temperature increases.

**Table 4.4 Stability Results for Wheat Farina, Temperature**

| Wheat Farina | S.BFE | SE | SI | FRI |
|---|---|---|---|---|
| 22°C | $14.43\pm0.06^{A}$ | $4.57\pm0.04^{A}$ | $0.96\pm0.00^{B}$ | $0.88\pm0.00^{B}$ |
| 52°C | $12.65\pm0.20^{B}$ | $3.94\pm0.08^{B}$ | $1.08\pm0.00^{A}$ | $1.20\pm0.06^{A}$ |
| 82°C | $12.06\pm0.02^{C}$ | $3.49\pm0.04^{C}$ | $1.07\pm0.02^{A}$ | $1.30\pm0.04^{A}$ |

As stated in the previous section, the Shear testing was difficult to obtain data for due to errors and faults. However, there were still discernible trends related to an increase in temperature to be seen. In this regard, farina behaved similarly to corn meal—increases in cohesion and UYS led to a marked decrease in flow function and increase in angle of internal friction. These trends matched visual observations of farina behaving as more of a solid mass and less of a free-flowing powder as it was heated for testing.

**Table 4.5 Shear Testing Results for Wheat Farina, Temperature**

| Wheat Farina | Cohesion | MPS | UYS | FF | AIF(E) |
|---|---|---|---|---|---|
| 22°C | $0.086\pm0.013^{C}$ | $10.60\pm0.26^{C}$ | $0.30\pm0.03^{A}$ | $35.74\pm2.85^{A}$ | $31.2\pm0.3^{C}$ |
| 52°C | $0.252\pm0.048^{B}$ | $11.33\pm0.09^{B}$ | $1.05\pm0.14^{B}$ | $11.57\pm1.24^{B}$ | $37.5\pm0.9^{B}$ |
| 82°C | $0.398\pm0.057^{A}$ | $12.00\pm0.12^{A}$ | $1.57\pm0.13^{C}$ | $7.59\pm0.61^{C}$ | $40.9\pm1.3^{A}$ |

Compressibility results lined up with the results obtained from the previous shear testing—definitively showing a correlation between increased cohesion and compression as temperature increased. When compared to corn meal, it can be seen that farina compresses nearly twice as much as corn meal at 15kPa of applied force at high temperatures. As the cohesion values would imply the opposite (with corn meal having a

higher cohesion value than farina), looking at other tests provided more insight—specifically the Stability Index from the Stability/Variable Flow Rate testing. Corn meal was shown to have a value much closer to 1.00, indicating a highly stable product, while farina was greater than 1.00, indicating a natural tendency to settle/compact. This natural tendency appeared to play a role in compression testing

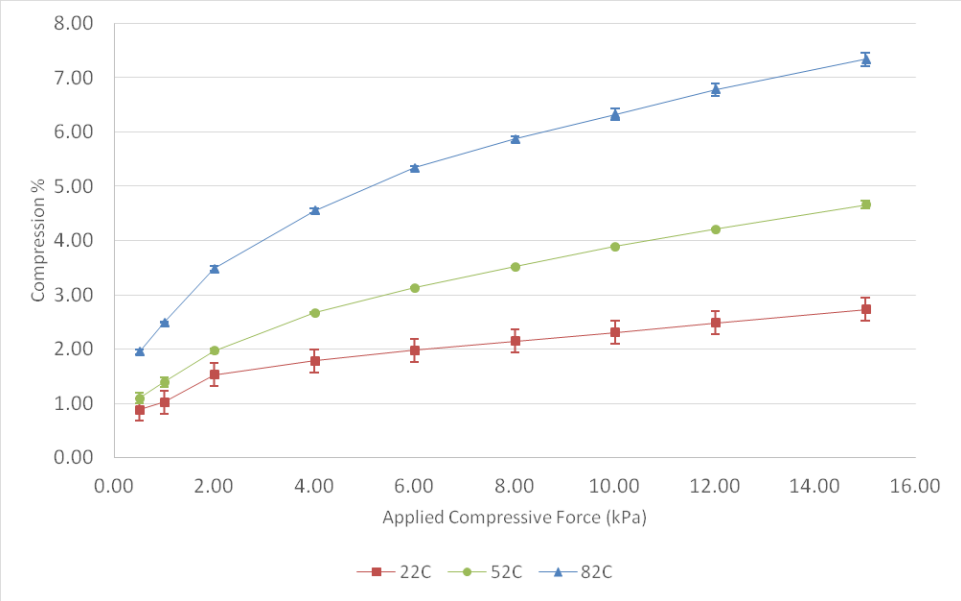


**Figure 4-2 Compressibility Results of Wheat Farina, Temperature**

Lastly, wall friction testing showed that an increase in temperature had a drastic impact on farina. Even though the results between 52°C and 82°C do not continue to increase, compared to room temperature, the impact is irrefutably strong. While corn meal was minimally impacted by temperature, the implication with these results (and visual observations of caked layers of farina on the wall friction disc at the completion of testing) are that a hot farina powder will most likely cake inside an extruder barrel.

**Table 4.6 Wall Friction Results for Wheat Farina, Temperature**

| Wheat Farina | WFA |
|---|---|
| 22°C | $6.4 \pm 0.1^{B}$ |
| 52°C | $36.7 \pm 1.1^{A}$ |
| 82°C | $38.6 \pm 0.5^{A}$ |

## 4.4 Conclusion

Despite farina requiring less energy per gram to flow in a confined environment, the drastic interaction between farina and surfaces would be a severe hindrance when flowing into an extruder barrel. Even though corn meal showed an increased energy requirement per gram, the lesser interaction with the barrel surface at increased temperatures (seen by the wall friction angle) would imply corn meal is a much more efficient powder for use if a starch-based powder is to be used in extrusion processing. Coupled with the results from the previous chapter, where corn meal was less resistant to flow in presence of moisture, the benefit of using corn meal over wheat farina as a primary ingredient in extrusion—specifically in single-screw extrusion, where conveying of raw materials is more difficult—is much clearer. As temperature and moisture are simultaneously introduced in preconditioning, further offline results to test these two parameters simultaneously would provide a more complete picture.

# Chapter 5 - Computer Simulations of Flow Properties of Starch-based Powders


## Abstract

During extrusion processing, material undergoes physical transitions from loose, granular material to a fluidized melt. While research has been done on fluid mechanics of the melted material, analysis of the flow of granular material is important in the feeding zone of the extruder barrel in order to understand flow (or lack thereof) of material when it is loosely agglomerated. To emulate the flow inside a fully-enclosed metal barrel, discrete element method analysis was performed to emulate four materials—corn meal, corn flour, wheat farina, wheat flour— to discern the influence of particle size and composition on these particulate flow properties, and an in-line validation of the materials with a 250RPM screw speed showed that wheat flour had a barrel fill of 72mm, while corn flour had a barrel fill of 221.8mm. Corn meal and wheat farina flowed so readily at this speed that no barrel fill was observed. These observations were then compared to the simulations, which were carried out on a fewer-particle scale.

Corn meal, corn flour, wheat farina, and wheat flour were used for flow analysis, all carried out at ambient temperature. EDEM version 2.7 was used to carry out simulation work, using generic, spherical shapes to replicate the particles of the aforementioned powders, while a Wenger X-20 single-screw extruder was used with a plexiglass window for in-line validation studies.

The results from the simulated particle flow showed trends similar to the in-line validations—corn meal and wheat farina flowed more freely than their finer-particle size materials of corn flour and wheat flour, verifying that even under simulated

circumstances, coarse food powders are better in single-screw extrusion applications than finer powders of the same material. A second run for corn meal and wheat farina, performed at a screw speed of 125RPM, yielded a barrel fill of 52.2mm for corn meal and 47.3mm for wheat farina, quantitatively showing an increased flow functionality for wheat products over corn products of similar particle size. These results were in line not only with the in-line validation, but with previous work done with experiments in previous chapters involving powder rheometry.

With these simulations shown to provide accurate trends within extrusion processing, the groundwork can be laid to simulate additional parameters such as the addition of heat to the metal barrel—something that cannot be done with the plexiglass window attached to the physical extruder. Further simulation work with more specific particle geometry or changes in screw profile will be able to provide additional accuracies to these trends, now that DEM modeling is verifiably a method to look within an extruder barrel that would otherwise remain unknown.

**5.1 Introduction**

The discrete element method (DEM) technique was developed by Cundall and Strack (1979) primarily to describe the mechanical behavior of discs and assemblies. Since its inception, the use of DEM has evolved from modeling small, two dimensional systems, such as chute flows and small hoppers, to modeling large industrial and geophysical systems (Cleary 2004). Recently, DEM has been extensively utilized to model granular food material production/handling processes (Boac 2014). The DEM technique has been used to model dragline filling (Coetzee 2009), screw conveyors (Cleary 2004), separation of particles on vibrating screens (Cleary 2004), bucket

elevators (Boac 2010), flow properties during discharge (Gonzalez-Montellano 2012), and more.

DEM is a numerical modeling technique that is based on the force-displacement laws of Newton's second law of motion. It involves monitoring particle interactions at each contact and modeling the particle motion for each particle (Boac 2014). The model generates particles that have physical and mechanical properties based on the input parameters given to the model. Depending on process conditions, DEM is able to model flow of individual particles, as well as their collisions, contacts, and the general interactions these particles undergo with other particles and the environment they were created in (Cleary 2001). These collisions and contacts cause the forces acting on each particle to change their position, velocity and characteristics. The resulting force is calculated by utilizing the contact models based on the force-displacement laws, with the resulting position and velocity data of the particles is calculated using Newton's second law of motion. This cycle of calculation of the resulting force, position and velocity of the particles is repeated for each particle for the defined number of time steps which results in simulating the flow of particles in a particle-machine system (Quist, 2012). Thus, the future of each particle is predicted by the repetition of an algorithm at every time interval (Gonzalez-Montellano 2012).

Contact models are used to determine the force-velocity-displacement during particle contact/collision as a mechanical system (Di Renzo 2004). The simplest mechanical system is a linear spring-dashpot model proposed by Cundall and Strack (1979) where the spring accounts for the elastic deformation and the dashpot accounts for the viscous dissipation. One of the common variations of the linear spring-dashpot model

is the more complex (and sound) Hertz-Mindlin and Deresiewicz model. It is based on the Hertz (1882) theory of elastic contacts of spheres in the normal direction and the Mindlin and Deresiewicz (1953) theory that gives the force-deformation relationship of contacting spheres in the tangential direction. However, due to the complexity of the model, it is considered to be time consuming in case of simulations involving granular flows and is not very common with DEM (Zhu 2007). Depending on the needs of the process, numerous simplified models based on the theories of Hertz and Mindlin and Deresiewicz have been developed and successfully used in DEM. Walton and Braun (1986) proposed a semi-latched force-displacement model in the normal direction based on the theory of Mindlin and Deresiewicz for cases on constant normal force in the tangential direction. Similarly, Thornton and Yin (1991) formulated a more complex model to simulate the tangential force by adopting Hertz theory for determining the normal force. Langston and Tuzun (1994) proposed a more intuitive model by using a direct force-displacement relationship for the tangential force while applying the Hertz theory for the normal force (Zhu 2007). All of the models mentioned above are direct simplifications of the Hertz and Mindlin and Deresiewicz contact theories and have successfully been used to study behavior of granular material (Zhu 2007). In a study by Di Renzo and Di Maio (2004), discussion and comparison of the contact force models used for simulation of collisions in DEM based granular flow was done. Although, there are contact models developed for non-contact forces or inter-particle forces that exist between particles and for particle-fluid interaction forces which can be used within DEM, the discussion of contact models is strictly limited to the applicability to this research work. Zhu et al. (2007) detailed a review of the theoretical development in terms of

understanding the microscopic mechanisms and interaction forces in discrete particle simulations of particulate systems. They have discussed the about the different types of contact models that have been developed over the past couple of years and successfully been applied in DEM.

In the DEM working software EDEM (v 2.6, DEM Solutions Ltd., Edinburgh, UK), there are different built-in contact models to suit the phenomena being simulated, with the simplest model referred to as the Hertz-mindlin (no-slip) contact model—a variant of the spring-dashpot model. It makes use of the elastic theory of Hertz for the normal contacts and no-slip solution of tangential contacts obtained from theory proposed by Mindlin and Deresiewicz (Di Renzo 2004).

### *5.1.1 Objectives*

1. Develop simulations of four starch-based powders (corn meal, corn flour, wheat farina, wheat flour) conveyed through screw conveyor system
2. Use imaging software to calculate powder dispersion within barrel to correlate with flow functionality in previous chapters
3. Utilize single-screw extruder to measure height of peaks and valleys inherent in the extrusion process during steady-state flow of four starch-based powders to validate functionality of offline measurements gathered in Chapter 2.
4. Utilize single-screw extruder to measure steady-state barrel fill of coarse corn and wheat food powders at increasing moisture content to validate functionality of offline measurements gathered in Chapter 3.

5. Utilize imaging software to calculate barrel fill percentage of all food powders at all moisture contents to correlate results on flow functionality of previous chapters.

## 5.2 Materials, Methods, and Variable Equations

### *5.2.1 Particulate Materials*

Corn meal, wheat farina, corn flour, and wheat flour were chosen to represent large and small particles for simulations. These particles were also suitable for in-line studies on a pilot-scale extruder, to corroborate the results of the simulations.

### *5.2.2 EDEM*

EDEM's simulations require multiple characterizations to determine particle behavior. Simple inputs in the system are the result of background research and calculations to provide a real-world application to a simulated environment. For the samples used in these simulations, the final values used for the parameters outlined here are compiled in a table in Section 5.3 – Results.

#### *5.2.2.1 Poisson's Ratio*

This ratio is a measure of the transversal expansion divided by the amount of axial compression. For a 1mm compression downward on a particle that results in a 0.1mm expansion to the sides, the Poisson's ratio would be 0.1. As this ratio is difficult to obtain in practical research on small particles, previously-published data was used, (Markauskas 2010; Sarnavi 2013; Weigler 2012)

#### *5.2.2.2 Coefficient of Static Friction*

The static friction coefficient between the particle and wall is measured using a laboratory device comprised of an open bottom container, test weight, and a pulley

system. A known weight of sample filled the open bottom container connected by the string-pulley system to a hanging cup. Weights were placed in the cup in small increments and the end point was determined when the container with sample moved for a corresponding increase in weight. The coefficient of static friction was calculated as the ratio of the weight required to move the sample to the weight of sample.

*5.2.2.3 Coefficient of Rolling Friction*

The coefficient of rolling friction, as described by Garnayak et al. (2008), is calculated based on an inclination of the surface until particles begin to roll. The tangent of this angle of inclination is determined to be the coefficient of rolling friction.

*5.2.2.4 Coefficient of Restitution*

Coefficient of restitution ($C_r$) is the change in kinetic energy of a particle when it collides with another object (static or kinetic). The importance of measuring coefficient of restitution is to accurately predict the behavior and motion of the particles after collision with other grain particles or with the steel screw or barrel face. To evaluate the coefficient of restitution against another material, a process outlined by Bharadwaj and Smith (2010) can be performed. Whereas a material is pressed into a tablet, and dropped from a known height ($H_0$), with the rebounded height ($H_1$) recorded and equation 5-1 used to calculate the coefficient of restitution.

$$C_r = \sqrt{\frac{H_1}{H_0}} \tag{5-1}$$

*5.2.2.5 Screw Setup*

A simple screw conveyor was used in the modeling of this simulation. A length of 1m and a diameter of 13cm, giving an L/D ratio of 8, no additional restrictions (kneading blocks, die plate, etc.) were created, allowing for free flow of material. The screw speed was set at 500RPM. Feed rate was set at 250kg/hr from a virtual "factory" to dispense particles into the feeding zone of the extruder.

*5.2.3 ImageJ*

This visual analysis software was used to determine a flow dispersion value in order to provide a uniform, objective comparison between the four simulations. As the barrel components were shaded blue and the particles were yellow, filtering all non-blue pixels gave the total number of pixels for the barrel; filtering all non-yellow pixels gave the total number of pixels of material. Dividing the number of yellow pixels by the total number of blue and yellow pixels, the flow dispersion for each material could be determined at any time snapshot in the simulation. The process was also used for the experimental runs of materials, analyzing snapshots once performance equilibrium was reached. Photos taken during these trials were modified to remove reflections and darken non-particulate portions of the extrusion barrel in order to more-accurately determine barrel fill through this software.

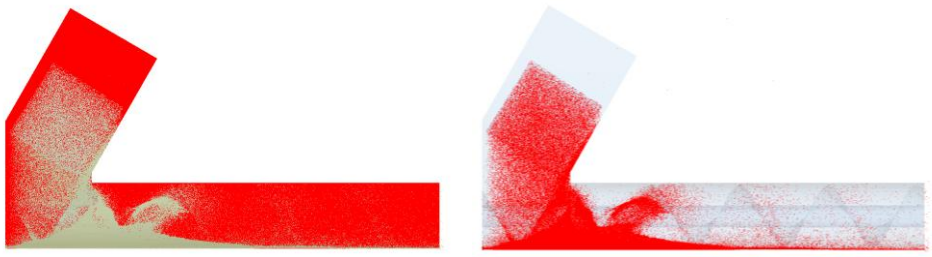

**Figure 5-1 Shading in ImageJ of barrel (left) and particulate material (right)**

### *5.2.4 Physical Screw Conveyor*

A Wenger X-52, single-screw extruder was used for in-line powder flow trials with a plexiglass window along one-third of the outer barrel. Four medium-sized kneading blocks were used to provide resistance and develop peaks of flowing material along the length of the barrel, whose height was then measured from the "valley" height of material prior to the kneading block restriction. Lower peaks correlated to a higher level of flowability, while a higher peak was indicative of a poorer-flowing material. Feed rate for corn meal and wheat farina trials was set at 80kg/hr with a screw speed of 125RPM. As there was no die plate at the end of the screw, a higher screw speed at this feed rate would force material through the barrel and not allow for peaks to develop, due to the increased gap between the plexiglass window and the screw. Due to the poor flow properties of corn flour and wheat flour, this screw speed was too slow and resulted in a clogged barrel. Subsequently, the screw speed was increased to 250RPM for these trials so that the measurable peaks were visible.

## 5.3. Results

In this section, EDEM simulations and ImageJ analysis are presented together, with inline trials presented separately. Links to YouTube videos for each run are provided in Appendix A

### *5.3.1 In-line Validation Study*

The results of the in-line study showed a correlation to the data developed in Chapters 2 and 3 regarding flow function for powders. As was established previously, a higher FF value indicated a more free-flowing powder. A powder that flows more readily was expected to have a reduced peak height at steam-locks and lesser barrel fill compared

to a powder that flows less readily. With the increased gap between the screw and plexiglass window compared to a traditional barrel, material was allowed to settle beyond the reach of the screw, so the height of the valleys was more exaggerated than during a typical, fully-enclosed run. Four peaks (one at each steam lock) and four valleys, along with the length of the barrel that was completely filled (from bottom to top) with material, were measured and recorded in the tables below.

Comparing the two coarse materials, wheat farina showed a steadier ebb and flow of material through the steam locks while corn meal was progressively more impacted by the flow restrictions caused by the steam locks. From Chapter 2, the FF of corn meal was found to be 4.94—a value that correlates to "free-flowing" qualities; the FF for wheat farina was found to be 18.47—a value that correlates to "highly free-flowing" qualities. The measured heights of the peaks and valleys fell in line with the results obtained by using the offline powder rheometer.

Due to the low FF of corn flour and wheat flour—2.36 and 3.29, respectively, the slow speed used for the coarse powders (125RPM) was insufficient to visualize the peaks and valleys, so the speed was increased to 250RPM. Peaks became visible at this speed, and measurements were taken. As both values for these powders fell into the "cohesive" category, the peaks, valleys, and barrel fill measured were all greater than their coarser counterparts. In the case of corn flour, the cohesive properties were great enough that both the fourth peak and valley were engulfed by the fill length from the end of the barrel.

Comparing the coarse and fine powders from each base materials yielded results that were to be expected—coarse corn meal flows better than corn flour, reflected in the

FF values of 4.94 and 2.36, respectively; wheat farina flows more freely than wheat flour, as was expected based on the FF of 18.47 and 3.29, respectively. While these results were unsurprising, the benefit of placing objectives results with known phenomena allowed for concrete analysis and comparisons and demonstrated the accuracy of offline tools such as the powder rheometer used in Chapters 2, 3, and 4.

**Table 5.1 Barrel fill and height of flow of food powders (in mm)**

| Material | Peak1 | Valley1 | Peak2 | Valley2 | Peak3 | Valley3 | Peak4 | Valley4 | Fill |
|---|---|---|---|---|---|---|---|---|---|
| C.Meal | 19.42 | 13.92 | 20.17 | 14.13 | 40.13 | 17.05 | 42.18 | 26.86 | 32.38 |
| W.Farina | 27.30 | 19.43 | 25.27 | 18.41 | 26.79 | 21.21 | 27.05 | 18.16 | 28.19 |
| C.Flour | 49.35 | 29.20 | 49.61 | 35.14 | 51.68 | 43.41 | 52.00 | 52.00 | 189.84 |
| W.Flour | 40.55 | 24.83 | 39.64 | 29.62 | 44.88 | 33.95 | 42.30 | 33.03 | 55.02 |

The hypothesis of increasing moisture content was that barrel fill would increase and the peaks and valleys would increase in height due to increased forces from liquid bridging. However, corn meal appeared to behave in an opposite manner in Chapter 3, with flow functionality and other values such as cohesion and internal angles of friction showing no statistical increase with increased moisture content or, in the case of AIF(E), decreased. Due to the complexity of these results, comparisons that solely utilized average flow functionality for each moisture level appeared to draw an incomplete picture of the validation study. Utilizing a combination of flow functionality, wall friction angle, and angle of internal friction, an understanding of these results was reached.

Looking at the height of peaks and valleys for corn meal in Table 5.2 it was not until more than halfway through the barrel—Valley #3—that measurements began to fall in line with anticipated trends. As FF did not clearly increase or decrease with moisture content in Chapter 3, the next value looked at was AIF(E), which showed a marked

decrease as moisture content increased. Combining that trend with Wall Friction values, which definitively increased with moisture content, the behavior of corn meal inside the extruder became more understandable.

In traditional extrusion processing, there are numerous variables that can be changed to influence the critical parameters of production. If more than one variable changes, and those changes have opposite influences, the final result cannot be determined solely by net plus/minus effects. In this trial, a decrease in AIF(E) occurs with a simultaneous increase in WFA, both of which affect particulate flow, and in opposite directions. Taking these changes into account while observing the values in the table below, it appeared that the counteracting forces worked at a similar rate in the presence of the additional moisture at the front end of the but the increased WFA became the dominant force at higher moisture content, with the steam locks exaggerating the increased friction between particle and surface so much that a reduced AIF(E) and comparable flow functionality were unable to maintain the evenness of flow observed in the first half of the barrel. The drastic increase in barrel fill from medium to high moisture content also strengthens this interpretation, as more particle buildup along the barrel face would be caused by increased wall friction.

**Table 5.2 Barrel Fill of Corn Meal at Increased Moisture Content (in mm)**

| Moisture | Peak1 | Valley1 | Peak2 | Valley2 | Peak3 | Valley3 | Peak4 | Valley4 | Fill |
|---|---|---|---|---|---|---|---|---|---|
| 13.13% | 19.42 | 13.92 | 20.17 | 14.13 | 40.13 | 17.05 | 42.18 | 26.86 | 32.38 |
| 15.50% | 31.27 | 14.43 | 30.72 | 14.43 | 31.64 | 20.73 | 45.89 | 35.16 | 38.76 |
| 18.14% | 27.61 | 14.37 | 27.61 | 21.56 | 46.71 | 33.28 | 47.65 | 38.57 | 86.00 |

One final reason for the slow development of heightened peaks with moisture content is that water added in the extruder is done at the beginning of the extruder,

preventing the even distribution of moisture that offline trials provided on the smaller sample size. In this trial, as the conveying action of the screw carried the water and corn meal forward, it mixed the two together to create more uniformity farther down the barrel, and leading to the trends observed in the latter section of the barrel.

The same multi-facet analysis used for corn meal at increasing moisture contents was used for wheat farina, as well. While flow functionality decreased substantially as moisture increased during offline analysis, the observed trend was more expected when accounting for increasing angles of internal friction and wall friction. The trend of increased peaks and valleys height definitively developed at the third peak, manifesting only slighter earlier in the barrel than its corn meal counterpart, although the runs at higher moistures were much more unstable, leading to surging, clumping, and a barrel fill that engulfed the final peak and valley, like corn flour in Table 5.2. Like corn meal, values in the first half of the barrel were varied and non-uniform but aligned with anticipated increases after the mixing action of the screw distributed water through the particulate. Unlike corn meal, however, the moisture increases were enough to partially activate the gluten matrix with the mixing action, which resulted in a much greater backfill of the barrel. Despite wheat farina having higher flow functionality ratings at increasing moisture contents (10.74, 6.11) than corn meal (5.15, 5.11) in offline testing, this surface development of the gluten matrix had a much stronger, adverse effect on flow during inline trials.

**Table 5.3 Barrel Fill of Wheat Farina at Increased Moisture Content (in mm)**

| Moisture | Peak1 | Valley1 | Peak2 | Valley2 | Peak3 | Valley3 | Peak4 | Valley4 | Fill |
|---|---|---|---|---|---|---|---|---|---|
| 13.73% | 27.30 | 19.43 | 25.27 | 18.41 | 26.79 | 19.21 | 27.05 | 18.16 | 28.19 |
| 15.25% | 26.84 | 15.49 | 25.29 | 16.92 | 29.92 | 19.70 | 41.32 | 29.03 | 42.69 |
| 18.00% | 25.27 | 16.04 | 24.80 | 14.10 | 33.84 | 23.09 | 52.00 | 52.00 | 165.31 |

*5.3.2 EDEM and ImageJ*

**Table 5.4 Simulation Variables for Materials**

| **Variable** | **Corn Meal** | **Corn Flour** | **Wheat Farina** | **Wheat Flour** |
|---|---|---|---|---|
| Poisson's Ratio | 0.20 | 0.25 | 0.20 | 0.25 |
| COSF (with Steel) | 0.40 | 0.48 | 0.35 | 0.32 |
| COSF (with Self) | 0.52 | 0.64 | 0.47 | 0.44 |
| CORF (with Steel) | 0.20 | 0.45 | 0.12 | 0.25 |
| CORF (with Self) | 0.25 | 0.55 | 0.20 | 0.52 |
| COR (with Steel) | 0.60 | 0.40 | 0.60 | 0.50 |
| COR (with Self) | 0.50 | 0.25 | 0.50 | 0.25 |

With the variables in Table 5.4, simulations were carried out until 1.50 seconds of simulated time was achieved. This duration was sufficient time to see material piled at the beginning of the screw and conveyed throughout a length of the barrel. Using EDEM's Analyst tab, snapshots were taken at 0.5 second intervals and imported to ImageJ. Pixel-counting analysis yielded the percentage of the cross-section view (seen in Figure 5-2, 5-3) that was particulate, which was compiled into Table 5.5.

**Table 5.5 ImageJ Flow Dispersion Percentage**

| Material | 0.0 seconds | 0.5 seconds | 1.0 seconds | 1.5 seconds |
|---|---|---|---|---|
| Corn Meal | 0% | 22.23% | 23.40% | 25.50% |
| Wheat Farina | 0% | 26.62% | 30.00% | 34.35% |
| Corn Flour | 0% | 18.71% | 20.39% | 22.90% |
| Wheat Flour | 0% | 17.36% | 19.18% | 21.90% |

Flow dispersion values determined from simulated particle flows were interpreted differently than barrel fill values derived from experimental flow trials, as the former analyzed particles after a specific time and the latter analyzed particles once steady-state performance was reached, regardless of time. Due to these key differences, a higher flow dispersion value generally indicated that material was able to flow through more of the barrel in a given time, which correlates to a higher flow functionality.

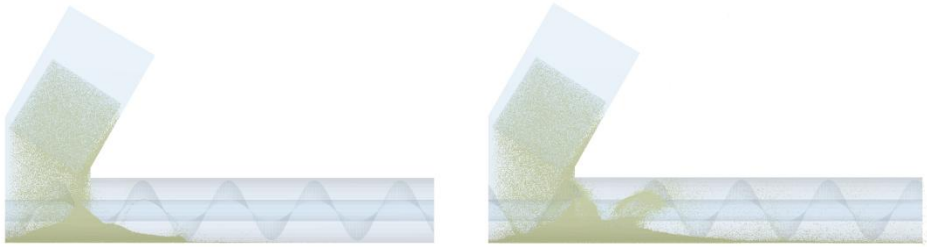

**Figure 5-2 Corn Meal (left) and Wheat Farina (right) simulated at 1.50 seconds**

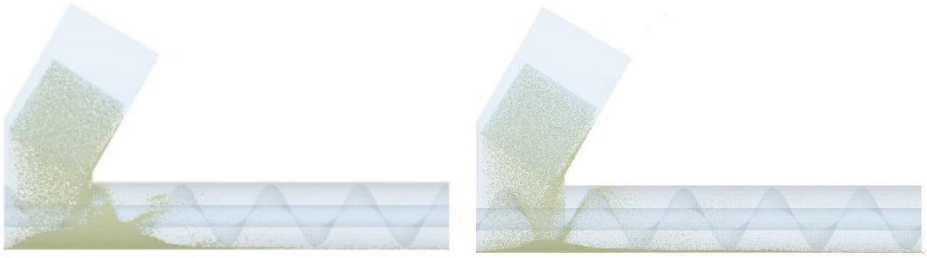

**Figure 5-3 Corn Flour (left) and Wheat Flour (right) simulated at 1.50 seconds**

As previously stated, a higher flow functionality value correlates to a lesser barrel fill percentage during in-line runs, shown in Table 5.6, where wheat flour and corn flour

fill a vast majority of the barrel and have the lowest FF values (see Chapter 2 for specific values). From Chapter 3, as moisture content increased for wheat farina, FF drastically decreased, which was observed in this validation trial and quantified through ImageJ. Also in that chapter, corn meal was observed to increase particle-particle forces although FF was not statistically impacted by these forces. That combination of values allows for a better understanding of the higher fill percentage value of corn meal at higher moistures. Despite this high fill percentage, corn meal flow was stable throughout the entire experiment unlike wheat farina, further reinforcing the importance of combining multiple test results to equate to actualities in the extrusion process.

**Table 5.6 Barrel Fill Percentage**

| **Material** | **Fill Percentage** |
|---|---|
| Wheat Flour | 71.34% |
| Corn Flour | 85.65% |
| Wheat Farina – 13.73% Moisture | 42.61% |
| Wheat Farina – 15.25% Moisture | 43.84% |
| Wheat Farina – 18.00% Moisture | 52.61% |
| Corn Meal – 13.13% Moisture | 43.18% |
| Corn Meal – 15.50% Moisture | 56.44% |
| Corn Meal – 18.14% Moisture | 65.19% |

The materials used in this experiment aligned with this developed correlation with one slight exception—wheat flour, which had a slightly higher FF value than corn flour, yielded a 1% lower flow dispersion value instead of an anticipated higher value. However, in the Chapter 2 results, the difference in these FF values was not statistically different, which tends to reinforce the accuracy of both powder rheometry and computer-simulated particle flows of powders utilized in extrusion processing.

## 5.4 Conclusion

Overall, the data collected during these validation studies tended to align with the offline data gathered from the powder rheometer in previous chapters. Data involving increased moisture strayed from offline expectations, although not so far as to appear erroneous. In addition to the difference in the mixing actions between offline and inline, the continuous input of water at a set rate inside the extruder allowed for consistent moisture content values to be targeted. However, for the powder rheometer trials, moisture was added and mixed prior to testing at ambient temperature and humidity, which would allow for evaporation over the course of the 10-20 minute testing procedure. Following the numerical trends observed with offline trials, this evaporation would decrease moisture content and increase flow functionality values (in the case of wheat farina), as well as associated changes in wall friction and angle of internal friction, compared to what would was observed in a steady-moisture state. These changes would allow for a predicted flow functionality that is higher than values observed in scaled-up extrusion systems. Due to the differences in the testing environment of Chapters 3 and 5, future studies should include moisture testing of samples after offline trials have been performed to discern moisture lost to the environment over the test duration. Accounting for this variation, however small, will provide more accurate numerical values while offline and correlate stronger with trends observed during inline studies.

# References

Abu-hardan, Madian, and Sandra E. Hill. 2010. “Handling Properties of Cereal Materials in the Presence of Moisture and Oil.” *Powder Technology* 198 (1):16–24. https://doi.org/10.1016/j.powtec.2009.10.002.

Anno Takahiko. 1981. “Studies on Heat-induced Aggregation of Wheat Gluten.” *Eiyo To Shokuryo* 34 (2):127–32. https://doi.org/10.4327/jsnfs1949.34.2_127.

Boac, J. M., Casada, M. E., Maghirang, R. G., & Harner, J. P., III. (2010). Material and interaction properties of selected grains and oilseeds for modeling discrete particles. Transactions of the ASABE, 53(4), 1201-1216

Boac, J. M., Kingsly, A. R. P., Casada, M. E., Maghirang, R. G., Maier, D. E. (2014). Applications of discrete element method in modeling of grain postharverst operations. Food Engineering Reviews, 6(3)

Burros, Byron C., Linda A. Young, and Paul A. Carroad. 1987. “Kinetics of Corn Meal Gelatinization at High Temperature and Low Moisture.” *Journal of Food Science* 52 (5):1372–76. https://doi.org/10.1111/j.1365-2621.1987.tb14085.x.

Caparino, O.A., C.I. Nindo, J. Tang, and S.S. Sablani. 2017. “Rheological Measurements for Characterizing Sticky Point Temperature of Selected Fruit Powders: An Experimental Investigation.” *Journal of Food Engineering* 195 (February):61–72. https://doi.org/10.1016/j.jfoodeng.2016.09.010.

Cundall, P. A., & Strack, O. D. L. (1979). Discrete numerican model for granular assemblies. Geotechnique, 29(1), 47-65

Coetzee, C. J., & Els, D. N. J. (2009). The numerical modelling of excavator bucket filling using DEM. Journal of Terramechanics, 46(5), 217-227

Di Renzo, A., & Di Maio, F. P. (2004). Comparison of contact-force models for the simulation of collisions in DEM-based granular flow codes. Chemical Engineering Science, 59(3), 525-541

Downton, Galen E., Jose L. Flores-Luna, and C. Judson King. 1982. "Mechanism of Stickiness in Hygroscopic, Amorphous Powders." *Industrial & Engineering Chemistry Fundamentals* 21 (4):447–51. https://doi.org/10.1021/i100008a023.

Egan, Harold, Ronald S. Kirk, Ronald Sawyer, and David Pearson. 1981. *Pearson's Chemical Analysis of Foods*. 8th ed. Edinburgh ; New York: Churchill Livingstone.

Freeman, R.E. 2000. "The Flowability of Powders - an Empirical Approach." *International Conference on Powder and Bulk Solids Handling*, 545–56.

Freeman, R.E., J.R. Cooke, and L.C.R. Schneider. 2009. "Measuring Shear Properties and Normal Stresses Generated within a Rotational Shear Cell for Consolidated and Non-Consolidated Powders." *Powder Technology* 190 (1–2):65–69. https://doi.org/10.1016/j.powtec.2008.04.084.

Freeman, Reg. 2007. "Measuring the Flow Properties of Consolidated, Conditioned and Aerated Powders — A Comparative Study Using a Powder Rheometer and a Rotational Shear Cell." *Powder Technology* 174 (1–2):25–33. https://doi.org/10.1016/j.powtec.2006.10.016.

Garnayak, D. K., Pradhan, R. C., Naik, S. N., & Bhatnagar, N. (2008). Moisture-dependent physical properties of Jatropha seed (Jatropha curcas L.). Industrial Crops and Products, 27(1), 123-129

Hertz, H. (1882). On the contact of elastic body. Journal of Pure and Applied Mathematics, 92, 156-171

Iqbal, T., and J.J. Fitzpatrick. 2006. “Effect of Storage Conditions on the Wall Friction Characteristics of Three Food Powders.” *Journal of Food Engineering* 72 (3):273–80. https://doi.org/10.1016/j.jfoodeng.2004.12.007.

Iveson, Simon M., and Neil W. Page. 2005. “Dynamic Strength of Liquid-Bound Granular Materials: The Effect of Particle Size and Shape.” *Powder Technology* 152 (1–3):79–89. https://doi.org/10.1016/j.powtec.2005.01.020.

Jenike, A.W. 1961. “Gravity Flow of Bulk Solids.” *Bulletin 108*, 1961.

Juliano, Pablo, Balasingam Muhunthan, and Gustavo V. Barbosa-Cánovas. 2006. “Flow and Shear Descriptors of Preconsolidated Food Powders.” *Journal of Food Engineering* 72 (2):157–66. https://doi.org/10.1016/j.jfoodeng.2004.11.032.

Langston, P. A., & Tuzun, U. (1994). Continuous potential discrete particle simulations of stress and velocity-fields in hoppers - Transition from fluid to granular flow. Chemical Engineering Science, 49(8), 1259-1275

Marston, J. O., E. Q. Li, and S. T. Thoroddsen. 2012. “Evolution of Fluid-like Granular Ejecta Generated by Sphere Impact.” *Journal of Fluid Mechanics* 704 (August):5–36. https://doi.org/10.1017/jfm.2012.141.

Mindlin, R. D., & Deresiewicz, H. (1953). Elastic spheres in contact under varying oblique forces. Journal of Applied Mechanics-Transactions of the ASME, 20(3), 327-344

Molenda, Mark, M.D. Montross, Josef Horabik, and I.J. Ross. 2002. “Mechanical Properties of Corn and Soybean Meal.” *Transactions of the ASAE* 45 (6):1929–36.

Peleg, M., C. H. Mannheim, and N. Passy. 1973. “FLOW PROPERTIES OF SOME FOOD POWDERS.” *Journal of Food Science* 38 (6):959–64. https://doi.org/10.1111/j.1365-2621.1973.tb02124.x.

Quist, J. (2012). Cone crusher modelling and simulation- Developement of a virtual rock crushing environment based on the discrete element method with industrial scale experiments for validation. Unpublished MS Thesis, Chalmers University of Technology, Goteborg, Sweden

Rabinovich, Yakov I., Madhavan S. Esayanur, and Brij M. Moudgil. 2005. “Capillary Forces between Two Spheres with a Fixed Volume Liquid Bridge: Theory and Experiment.” *Langmuir* 21 (24):10992–97. https://doi.org/10.1021/la0517639.

Riaz, Mian N., ed. 2000. *Extruders in Food Applications*. Lancaster, Pa: Technomic Pub. Co.

Rogé, B, and Mohamed Mathlouthi. 2000. “Caking of Sucrose Crystals: Effect of Water Content and Crystal Size.” *Zuckerindustrie* 125:336–40.

Stasiak, Mateusz, and Mark Molenda. 2004. “Direct Shear Testing of Flowability of Food Powders.” *Research in Agricultural Engineering* 50 (1):6–10.

Stasiak, Mateusz, Mark Molenda, Ireneusz Opalinski, and Wioletta Blaszczak. 2013. “Mechanical Properties of Native Maize, Wheat, and Potato Starches.” *Chech Journal of Food Science* 31 (4):347–54.

Stoklosa, Adam M., Rebecca A. Lipasek, Lynne S. Taylor, and Lisa J. Mauer. 2012. "Effects of Storage Conditions, Formulation, and Particle Size on Moisture Sorption and Flowability of Powders: A Study of Deliquescent Ingredient Blends." *Food Research International* 49 (2):783–91. https://doi.org/10.1016/j.foodres.2012.09.034.

Teunou, E, and J.J Fitzpatrick. 1999. "Effect of Relative Humidity and Temperature on Food Powder Flowability." *Journal of Food Engineering* 42 (2):109–16. https://doi.org/10.1016/S0260-8774(99)00087-4.

Thomas, J., and H. Schubert. 1979. "Particle Characterization." *Partec* 79:301–19.

Wallack, David A., and C. Judson King. 1988. "Sticking and Agglomeration of Hygroscopic, Amorphous Carbohydrate and Food Powders." *Biotechnology Progress* 4 (1):31–35. https://doi.org/10.1002/btpr.5420040106.

# Appendix A - Supplementary Pictures and Videos

## A.1 Offline Equipment Used in Testing


**Figure A-1 FT4 Powder Rheometer**

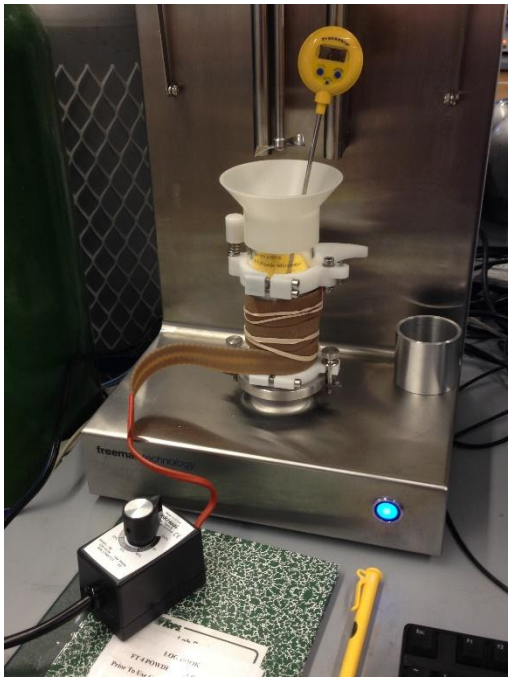

**Figure A-2 Thermal Modification of Aluminum Cylinder, with Thermometer (Ch.4)**

## A.2 Inline Experiments

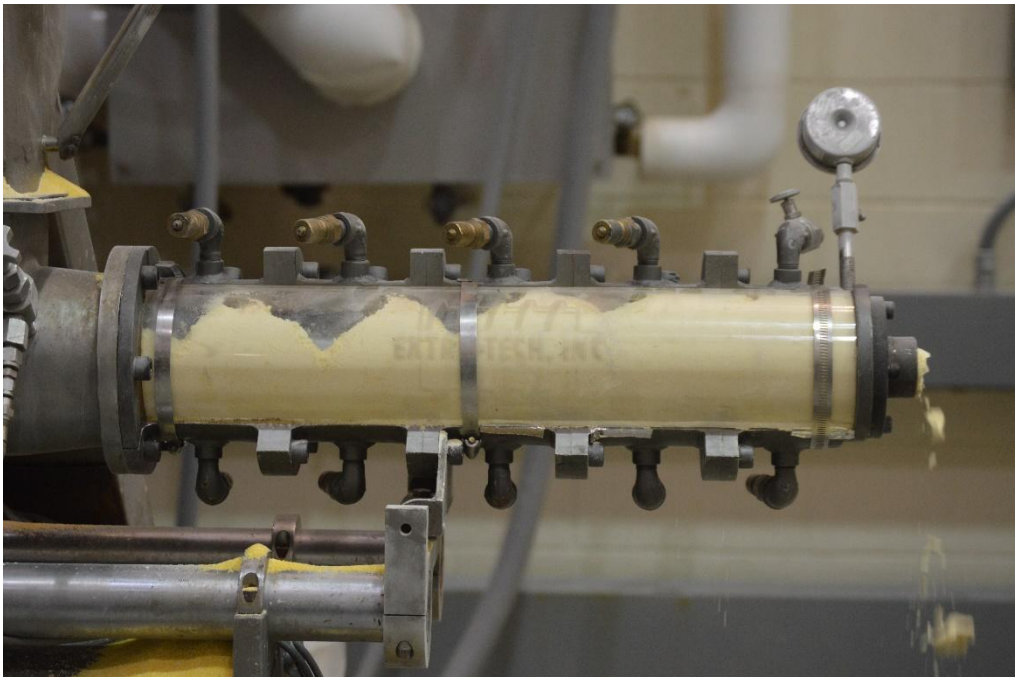

**Figure A-3 Corn Flour at Steady State**

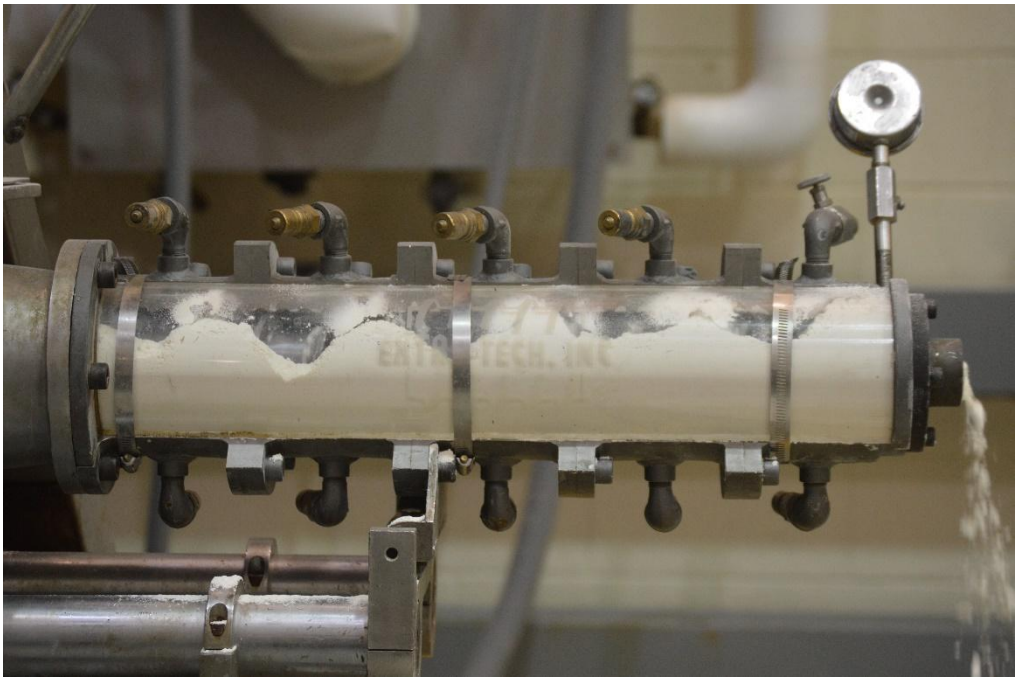

**Figure A-4 Wheat Flour at Steady State**

**Figure A-5 Corn Meal at Steady State (13.13% Moisture)**

**Figure A-6 Corn Meal at Steady State (15.50% Moisture)**

**Figure A-7 Corn Meal at Steady State (18.14% Moisture)**

**Figure A-8 Wheat Farina at Steady State (13.73% Moisture)**

**Figure A-9 Wheat Farina at Steady State (15.25% Moisture)**

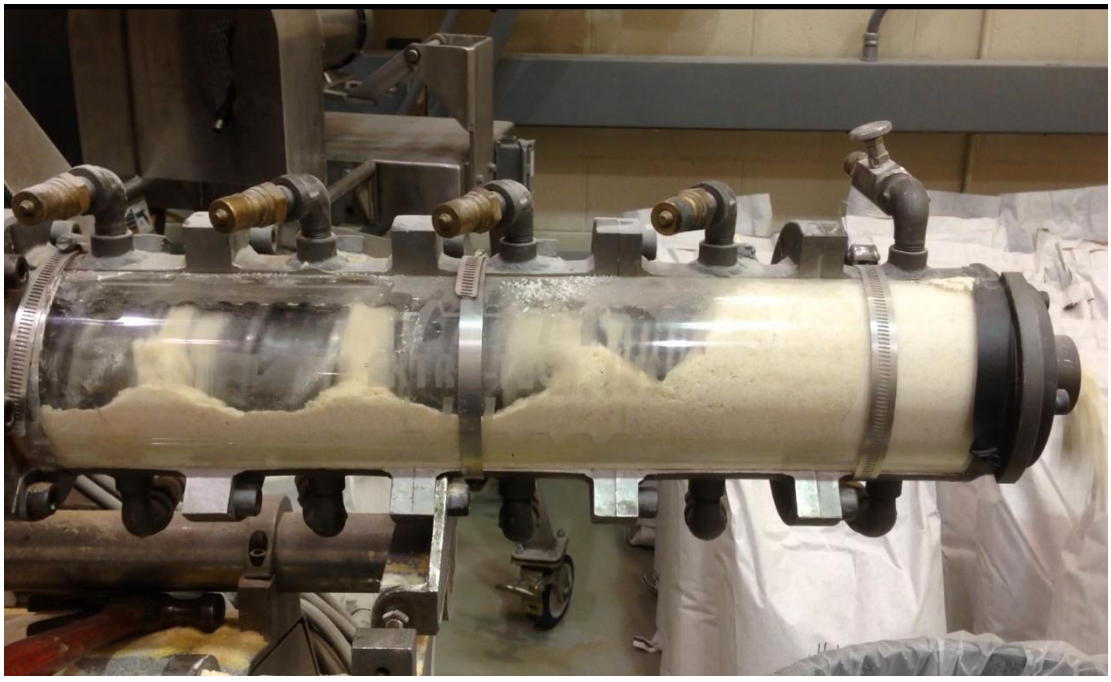

**Figure A-10 Wheat Farina at Steady State (18.00% Moisture)**

## A.3 Video Links

### *A.3.1 Inline Validation*

Corn Flour Video – https://youtu.be/p5XrFwT5DP4

Wheat Flour Video – https://youtu.be/Bt8uJ63-9fA

Corn Meal (13.13% Moisture) Video – https://youtu.be/qdsS2b5REno

Corn Meal (15.50% Moisture) Video – https://youtu.be/wEYcZvaeiCI

Corn Meal (18.14% Moisture) Video – https://youtu.be/UQSHaxRN4M4

Wheat Farina (13.73% Moisture) Video – https://youtu.be/r8L9cvlXeO8

Wheat Farina (15.25% Moisture) Video – https://youtu.be/lMol-wzCdvM

Wheat Farina (18.00% Moisture) Video – https://youtu.be/CC5wFbF2Pew

### *A.3.2 Computer Simulation*

Corn Flour Simulation Video – https://youtu.be/Z5Y7Nx4kntc

Wheat Flour Simulation Video – https://youtu.be/sMfM696p-p8

Corn Meal Simulation Video – https://youtu.be/JP2doTVSyms

Wheat Farina Simulation Video – https://youtu.be/hrZCygLfNjg